UNIVERSITY OF BIRMINGHAM

HYDROGEN SORPTION IN PALLADIUM DOPED MICROPOROUS MATERIALS

by

PHILIP HAMILTON

A thesis submitted to the University of Birmingham for the degree of Masters in Research (MRes)

School of Metallurgy & Materials
College of Engineering & Physical Sciences
University of Birmingham
B15 2TT
United Kingdom
September 2009

ABSTRACT

This research investigated “hydrogen spillover” which has been suggested to improve the hydrogen uptake of bridged and chemically doped porous materials at room temperatures. XRD, Temperature Programmed Desorption and hydrogen sorption measurements were used to characterise the as-received and palladium doped porous materials.

The hydrogen uptakes of as-received Maxsorb (activated carbon), Black Pearls (carbon furnace black) and MOF-5 (metal organic framework) were all very low (<0.16 wt.%) at room temperature and 16 bar. Bridging the Black Pearls and Maxsorb carbon samples with 5 wt.% Pd/C resulted in fractionally higher hydrogen uptakes (0.01 wt.%). These results bore a closer resemblance to a physical mixture of Pd and carbon which suggested that the bridges had not been formed and spillover was not occurring.

A higher wt.% Pd chemically doped carbon showed an initial rapid hydrogen uptake (0.03 wt.% at <1 bar) followed by a shallower near linear uptake above this pressure. The hydrogen uptake seemed more consistent with palladium and carbon sorbing independently, rather than hydrogen spilling over from palladium to carbon giving enhanced uptake. However, good contact between Pd and carbon must be established and the result must be replicated to confirm its validity in the face of much contrary literature.

Soli Deo Gloria

ACKNOWLEDGEMENTS

I would like to thank my supervisor Dr. David Book for his knowledge, enthusiasm and positive approach to this research, Dr. Allan Walton for his perseverance, discussions and instruction especially on the IGA & HTP, Phil Chater for his assistance in the chemistry department and the Hydrogen Research Group for providing an enjoyable atmosphere to study in. I also thank Alvaro Amieiro and the rest of the staff at Johnson Matthey for their discussions and assistance in the synthesis of palladium doped microporous samples. Furthermore, I would also thank my fiancée, family and friends for their support and encouragement throughout the year. Finally, my thanks to Birmingham University for paying my tuition fees and for the generous financial support of the Engineering and Physical Sciences Research Council (EPSRC).

TABLE OF CONTENTS

1 - INTRODUCTION

1.1 - BACKGROUND

There are growing pressures to progress from a fossil fuel based economy to an alternative, more sustainable energy economy. The multiple drivers for change in energy economy include adverse climate change, negative health effects, resource depletion and energy security concerns.

1.1.1 - Adverse Climate Change

Global greenhouse gas emissions due to human activities have grown since pre-industrial times by 70% between 1970 and 2004[1]. Although the CO_2 levels do naturally rise and fall, the current atmospheric concentrations of 387 ppm determined from ice cores far exceed the natural range of the past 750,000 years[2]. Although climate predictions are dependent on which climate model is used and assumptions made about future global emissions, the Intergovernmental Panel on Climate Change estimates a global average temperature rise of 1.8 - 4°C this century[1]. There is also increasing statistical confidence in projected increases in extremes of weather such as droughts, heat waves and floods.

1.1.2 - Negative Health Effects

Air pollution such as SO_2, NO_2, O_3 and particulate matter from fossil fuel combustion have been linked to cardiovascular and respiratory problems[3]. Continued global warming would

increase the spread of disease due to elevated temperatures and through damaged sanitation systems by extreme weather events. Rising sea levels as a result global warming pose a serious risk to both developed and undeveloped coastal populations such as London, New York, Shanghai and the Ganges delta in Bangladesh.

1.1.3 - Resource Depletion

There are a variety of "peak oil" models that predict the maximum rate of global oil production, after which, the production enters into terminal decline. Many models suggest that we are already at, or have nearly reached peak oil. This problem is further exacerbated by the projection of world marketed energy consumption increasing by 50 % from 2005 to 2030 if current laws and policies remain unchanged[4]. This does not take into account the additional expected demand from developing countries such as China and India. Much of the deviation between models comes from confusion surrounding world oil reserves.

1.1.4 - Energy Security

Energy resources such as coal, gas, oil and uranium are not uniformly distributed across continents and countries which creates a dependence on a few countries for energy. The changeable energy policies of distributing governments are not conducive for a long term and secure energy supply. Recent instability in Iraq, Venezuela and Nigeria, and the arguable use of oil for political influence in Russia and the Middle East contribute to feelings of energy uncertainty[5].

The UK government recently released a review[6] on the economics of climate change that concluded that the benefits of strong, early action on climate change outweigh the costs of doing nothing now and that there is still time to avoid the worst economic impacts of climate change, if strong action is taken now.

1.2 – A FUTURE ENERGY ECONOMY

Hydrogen has long been proposed by many as a replacement energy carrier for a future energy economy. This is because there are potentially abundant supplies and it can store large amounts of energy, which can be released cleanly without harmful emissions. These features make hydrogen particularly attractive when considering the drivers for change as outlined above. Furthermore the increase in energy generation from renewable sources requires forms of energy storage as production fluctuates hugely with solar, wind and tidal activity. The energy stored in hydrogen can later be released through electrochemical fuel cells that recombine hydrogen with oxygen, with no emissions of harmful gases. The two main types of fuel cell are Solid Oxide Fuel Cells (SOFC) and Polymer Exchange Membrane Fuel Cells (PEMFC) which is illustrated in Figure 1.1 below.

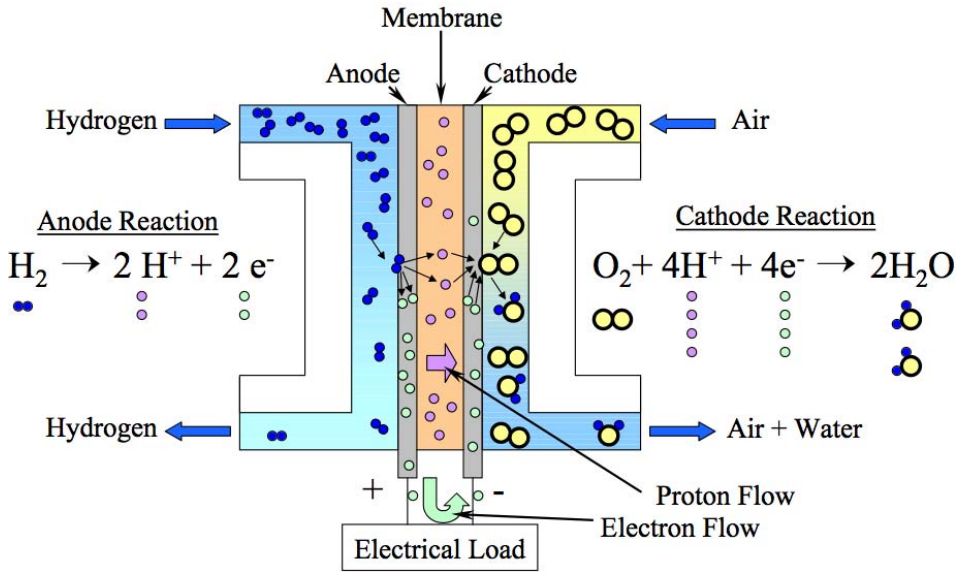

Figure 1.1 shows a Proton Exchange Membrane (PEM) fuel cell

1.2.1 - Production

Although there are large amounts of hydrogen in the world, it naturally exists being chemically bonded to other elements e.g. oxygen in H_2O, rather than as a free gas. Production is currently achieved primarily through steam reforming of natural gas but is also possible by coal gasification. Electrolysis and other novel methods including photolytic processes and biological methods are also currently possible. Future methods of hydrogen production include high temperature electrolysis, which offers increased efficiency as some of the energy required to split hydrogen and oxygen is provided by the higher temperatures. These high temperatures could be generated from high temperature energy generation plants including nuclear, concentrated solar and geothermal. Alternatively, thermochemical processes could potentially be taken advantage of which may use the sulphur-iodine cycle to produce hydrogen[7].

1.2.2 - Utilisation

Currently, the vast majority of hydrogen is either used in agriculture in the production of ammonia for fertilizer through the Haber process, or in the oil industry to convert heavy crude oil distillation fractions to lighter hydrocarbons through hydrocracking. Future utilisation of hydrogen could include long term energy storage for balancing varying supply from low carbon/renewable energy sources with varying demand, a replacement for fossil fuels in the transport and domestic sectors and in portable electronics such as mobile phones and laptops which could be powered by fuel cells.

1.2.3 – Safety

Despite the advantages of using hydrogen as a fuel source, there are some potential safety concerns. These however, are to be expected from all good fuels that are capable of carrying large amounts of energy. The disadvantages are that hydrogen has a very wide explosive limit in air (4 – 75%), low ignition energy, a clear flame in daylight and is easily leaked. This final characteristic could also be seen as an advantage as hydrogen gas disperses rapidly away from the source of the leak and it is also lighter than air, which means that it will not pool as a liquid fuel would. Changing public perception through increasing public awareness of the different dangers associated with hydrogen still needs to be properly addressed before hydrogen will be accepted as a safe energy carrier.

In summary, before a hydrogen/electric economy can be established, issues such as mass production, storage, distribution and safety must be overcome.

1.3 - HYDROGEN STORAGE

The storage of hydrogen is one of these primary challenges to its successful implementation in an alternative energy economy that includes both mobile and static applications. Although hydrogen has an excellent gravimetric energy density of around 120 MJ/kg, the volumetric energy density is substantially poorer in comparison to current fuels: 1 kg of H_2 occupying 11 m^3 at STP. To put this in perspective, about 4 kg of stored hydrogen would be necessary to fuel a small car for 400 km. Consequently a technique by which the hydrogen molecules can be packed more closely is needed. The current target set by the US Department Of Energy (DOE) for a vehicular hydrogen storage system is 6 wt.% by 2010. The ideal hydrogen storage method has a good gravimetric density and volumetric density, equilibrium properties near ambient temperature and pressure, is reversible over many cycles, has fast transfer rate and is stable in air. Further considerations are costs, recycling and charging infrastructures. Hydrogen can be stored in three states of matter as a gas, liquid or solid forms. The best method of storage is often dependent on the intended application. Transport applications are often the most stringent as they require both high gravimetric and volumetric energy densities.

1.3.1 – Compression

As hydrogen is a gas at room temperature and pressure it can be relatively easily compressed and stored in cylinders such as that shown in Figure 1.2. These usually have a protective layer, a carbon fibre shell for strength and a polymer liner to prevent gas leakage.

Figure 1.2 shows a compressed hydrogen gas storage system for an automotive application

The benefits of compression are that it is a well established technology and is compatible with the existing chemical industry infrastructure. It has been used to store gases including hydrogen for a many years and it has fast refueling and discharge rates. The problems associated with this process are that a proportion (15 %) of energy is lost in compressing the gas, reducing overall efficiency and that pressure reduction steps must be introduced to be manageable for use in a fuel cell. Additionally, the size of storage still results in the loss of boot storage space. Whilst the pressure at which hydrogen can be stored is increasing through improving technology reducing the space required this does raise some important safety concerns about the large amounts of energy released should a puncture occur.

1.3.2 – Liquid Storage

Liquefaction of hydrogen at 20 K gives improved volumetric density, but the associated energy loss to achieve this is even higher (up to 30 %). This gives higher energy density and does not necessarily require high pressure, although the use of additional pressure gives a volumetric density of nearly twice that of compressed hydrogen. Disadvantages are a more complex design requiring pressure release valves, difficulty in handling, still a large storage

space being required for the system and 'boil off' over relatively short periods of time. The extent of boil off is dependent on size, shape and thermal insulation properties of the storage vessel, an example of which is shown in Figure 1.3. Additional safety concerns include those associated with cryogenic liquids. This method of storage is arguably limited to applications where the cost of hydrogen is irrelevant and the gas is used within a short period of time, such as in space shuttles.

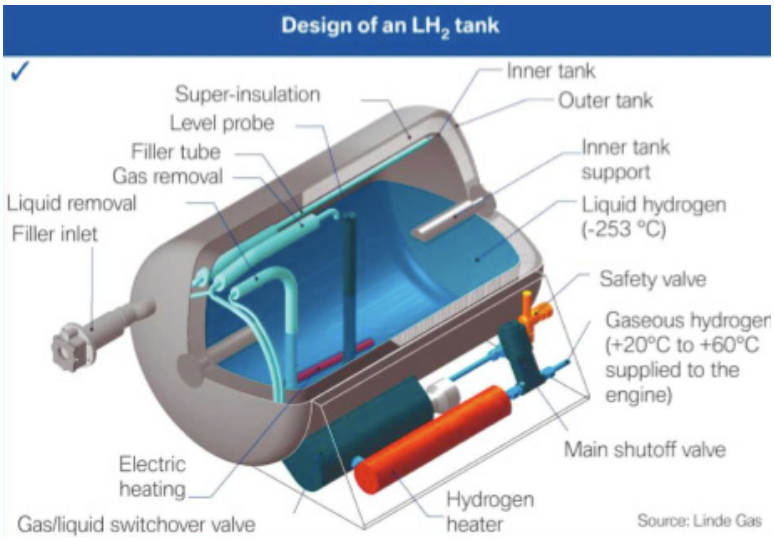

Figure 1.3 shows a liquid hydrogen storage system

Another form of liquid storage is water itself, which stores about 11.1 wt.% H_2. However it requires a substantial amount of energy for its decomposition to hydrogen and oxygen. This can also be achieved by reacting metals and chemical compounds with water e.g. $2Na + 2H_2O \Rightarrow H_2 + 2NaOH$. When lithium is used as the reacting metal, 6.3 wt.% of stored hydrogen is attainable. The main problems with this approach are reversibility and the reduction and recovery of the metal hydroxide.

1.3.3 - Solid State Storage

Solid state storage of hydrogen can be achieved by "binding" the hydrogen to other materials. There are two ways by which this can be achieved; chemisorption and physisorption.

1.3.4 – Chemisorption

Chemisorption of hydrogen is possible by using metal hydrides (MgH_2) and complex hydrides (e.g. $LiBH_4$). Hydrogen is dissociated at the surface forming H ions that diffuse into the material and form ionic, covalent or metallic bonds. The difficulties associated with this type of storage method area high enthalpy of formation, which requires high temperatures for desorption in order to break the strong bonds, slow desorption kinetics and a high reactivity toward air and oxygen. Due to the very high proportion of metal atoms in these storage materials the gravimetric energy densities are generally poorer for metal hydrides. However, they do have potential for stationary applications and where weight is not a significant issue such as submarines or barges. Complex hydrides such as $LiBH_4$ are usually made from alkaline metal elements in the first three groups of the periodic table. They differ from metal hydrides in that they change to a ionic and/or covalent compound on absorption. They include alanates (AlH_4^-), amides (NH_2^-), imides and borohydrides (BH_4^-). They have advantages of being lightweight and more importantly the ability to generally bind two H atoms per metal/non metal. This results in very good volumetric and gravimetric densities, for example $LiBH_4$ contains around 18 wt.% H_2. Unfortunately due to the stronger type of bonding, the hydrogen desorption temperature is too high and the desorption kinetics too slow for practical use.

1.3.5 – Physisorption

Physisorption can be achieved through a range of high surface area materials including zeolites, metal organic frameworks, polymers with intrinsic microporosity and a wide range of carbons. This process takes advantage of the attractive van der Waals forces between molecular hydrogen and the surface of the storage material for adsorption. This storage method has good reversibility and fast kinetics. However due to the low enthalpy of adsorption (5-10 kJ/mol) linked with weak bonding these materials require low temperatures (~77 K). To adsorb significant quantities of gas the materials require very high surface areas (~1000 m^2/g) and small pore sizes.

Carbon materials have long been considered for hydrogen storage as they have low densities, large diversity of structural forms, extensive pore structures and are able to be widely modified[8]. There were some initial extravagant claims[9,10], but further research has shown that there is no unique mechanism operating other than the relationship between increasing hydrogen uptake with apparent surface area and micropore volume[11]. The maximum uptake recorded for high surface area zeolite-like carbon is 6.9 wt% at 77 K and 20 bar[12]. The storage properties of carbon aerogels and foams, which are highly porous solid materials with extremely low densities, are also being investigated. However, as with all low density materials, these will have very low volumetric storage densities.

BLACK PEARLS 2000 used in this investigation (as seen in Figure 1.4) is a type of carbon black that can be further categorized to a furnace black or carbon soot due to the method of manufacture. The furnace method of production involves the incomplete combustion of oil

based products. They are primarily used for rubber reinforcement in tyres and also as black pigment.

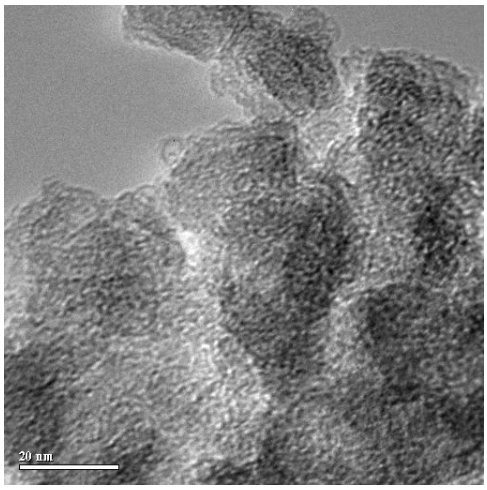

Figure 1.4 TEM image of Black Pearls 2000 obtained from Cabot Corporation Ltd.[14]

This type of carbon black has been previously used for Pd/C catalysts[13] and as a hydrogen storage material[14] (see Figure 1.5). It has an external surface area, which means that the surface area is not as high as those with both an internal and external surface area. The BET surface area given by suppliers is 1475 m^2/g, but previous research at the University of Birmingham has found it to be 1346 m^2/g[14].

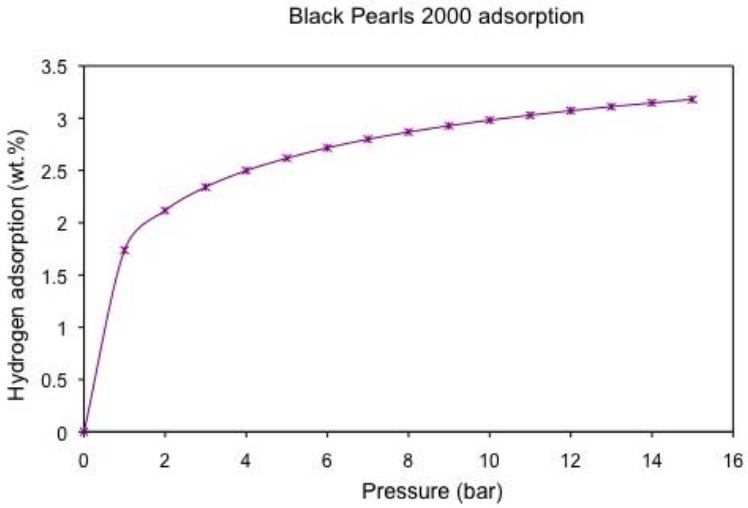

Figure 1.5 Hydrogen adsorption on as received Black Pearls 2000 at 77 K measured on a Hiden IGA system upto 15 bar [14]

MAXSORB was also used as a hydrogen storage material. This is a high surface area (>3000 m^2g) activated carbon. It is produced by mixing various kinds of petroleum coke with excess KOH, dehydrating at 673 K and activating at about 973 K in an inert atmosphere[15]. It has a mean pore diameter of 2.12 nm and a true density of 2.19 g/cm^3[3,16]. Due to its high surface area and small pore size it has been investigated for use as a hydrogen storage material (see Figure 1.6) and has shown some improvement with Pd doping.[17]

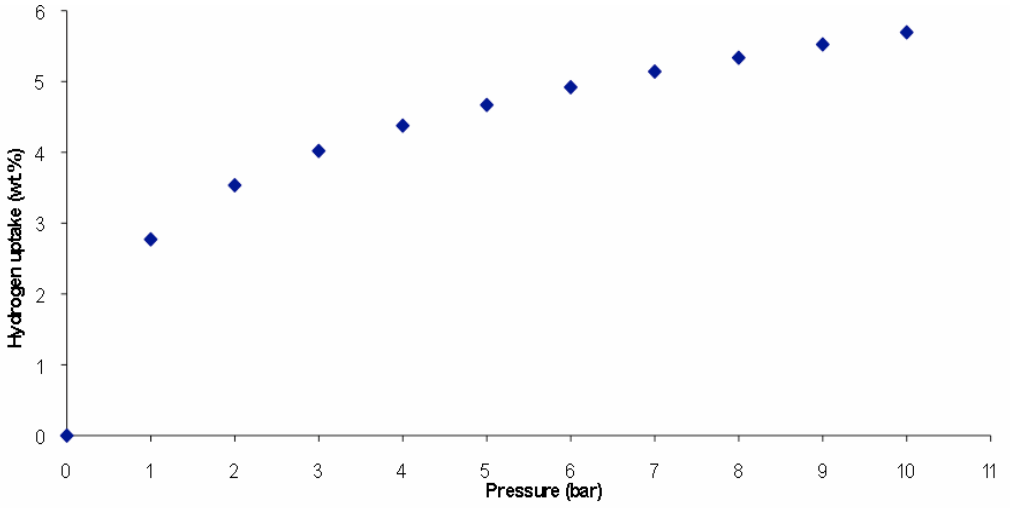

Figure 1.6 Hydrogen adsorption on as-received Maxsorb at 77 K measured on a Hiden IGA system upto 10 bar [18]

Metal organic frameworks (MOF) have more recently been reported as hydrogen storage materials[19]. These are synthesised structures made from a combination of organic linkers and metal corners. The structure can be extensively tailored by altering the linkers and corners and consequently its adsorption properties and over 5000 have been developed so far. They can have exceedingly high intrinsic surface areas and therefore potentially large hydrogen storage capacities. Currently surface areas of up to 5500 m^2/g and storage of ~7.5 wt.% H_2 at 77 K and 70 bar have been recorded in MOF-177[20]. This investigation will use MOF-5, which has

previously been characterized at low temperatures at the University of Birmingham as seen below in Figure 1.7.

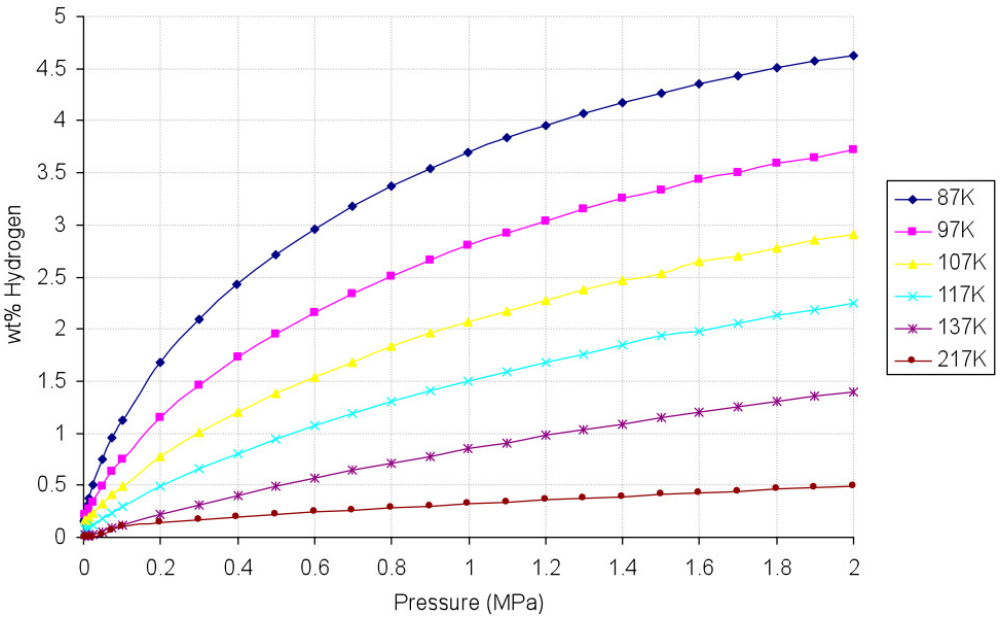

Figure 1.7 Hydrogen adsorption on MOF-5 at 87 to 217 K measured on a Hiden IGA system upto 2 MPa[21]

Figure 1.8 below shows the temperature for significant hydrogen release by present hydrogen storage materials and where the ideal 2010 US Department Of Energy complete system target is situated. The actual storage material will have to 30-50 % higher to compensate for the weight of the complete system. Although the storage wt.% of current bridged materials is too low, they do release hydrogen within the ideal temperature zone.

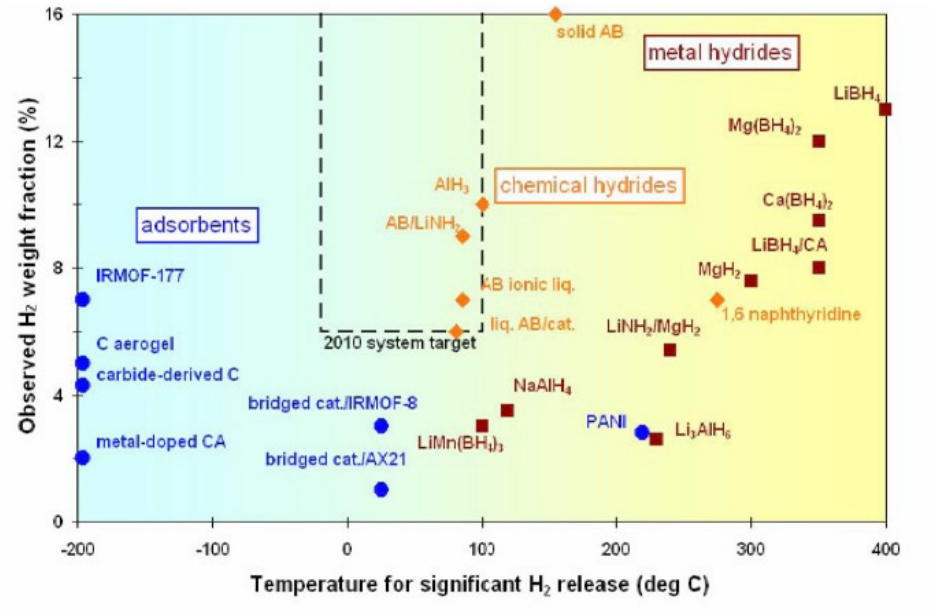

Figure 1.8 Hydrogen wt.% vs release temperature[22]

1.4 – GAS ADSORPTION & RELIABILITY OF MEASUREMENT

Adsorption is the condensation of gas on the surfaces of a material. The amount of gas adsorbed is dependent on the properties of the solid and gas, pressure and temperature. An adsorption isotherm can be achieved when the amount of gas adsorbed is measured versus the pressure of gas at a fixed temperature. There are six types of isotherm, but the Langmuir Type I isotherm (see Figure 1.9) is characteristic of the physisorption of gas onto microporous solids. This shows a sharp initial increase followed by a long plateau as the micropores and surface sites become filled.

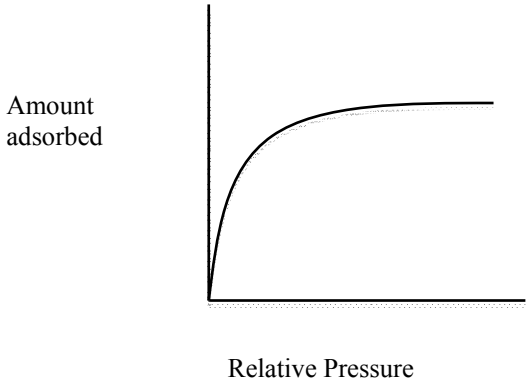

Figure 1.9 Type I isotherm of the adsorption of a gas onto a typical microporous solid

The practical measurement of hydrogen storage in materials still needs to be improved. Recent round-robin testing[23] in 2008 (see Figure 1.10) was carried out on a carbon standard material by members of the EC FP6 "Novel and Efficient Solid State HYdrogen storage systems" (NESSHY) project.

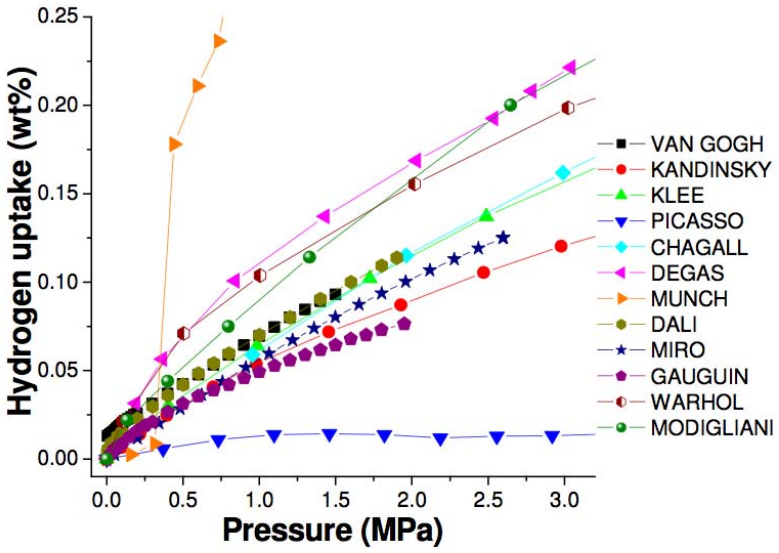

Figure 1.10 Variation in room temperature hydrogen uptake isotherms for a carbon standard, measured by various research groups involved in the "Novel and Efficient Solid State HYdrogen storage systems" (NESSHY) project using gravimetric and volumetric systems[23]

These results above clearly show a wide scatter in hydrogen uptake at low pressures and ambient temperatures. This shows that there are still a number of methodological issues to be resolved before hydrogen uptake measurements of high surface area carbons can be reliably reported.

1.5 – SPILLOVER

A mechanism of hydrogen spillover has recently been proposed for high surface area materials that has suggested that the adsorption enthalpy can be increased to be in the region between physisorption (<10 kJ/mol) and chemisorption (~50 kJ/mol)[24]. If spillover is proved to be correct then enhanced hydrogen adsorption at near ambient temperature and pressure would be possible. Spillover has been defined[25] as the transport of an active species sorbed or formed on a first phase onto another phase that does not under the same conditions sorb or form the species. A variety of catalysts have been utilised to increase hydrogen storage, however palladium has shown the best catalytic effect for the dissociation of hydrogen[26]. Figure 1.11 below shows a proposed mechanism for hydrogen spillover where H_2 dissociates on the metal particle and protons migrate via a "bridge" to the adsorbent material.

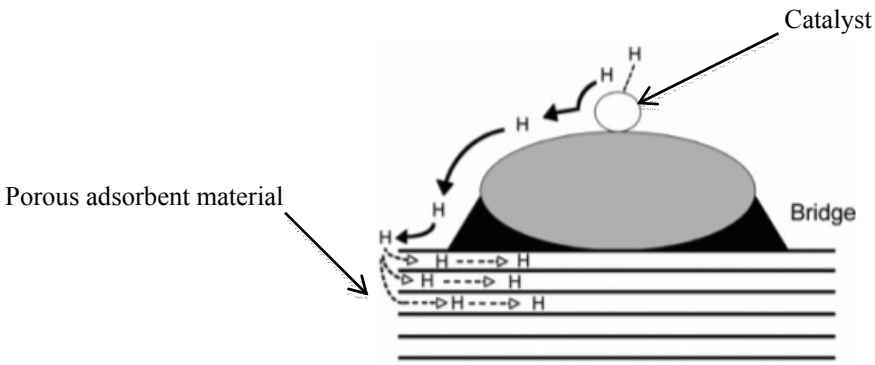

Figure 1.11 Proposed spillover mechanism[27]

2 - LITERATURE REVIEW

This literature review will focus on the hydrogen spillover mechanism and its specific application to hydrogen storage materials in carbons and metal organic frameworks.

2.1 - BACKGROUND

Although "spillover" has been well documented in catalytic literature over the last few decades, the exact mechanism and its significance is still not well understood. It has been defined in an extensive review[25] as the transport of an active species sorbed or formed on a first phase onto another phase that does not *under the same conditions* sorb or form the species. Spillover is one fundamental step in a series of mechanistic and kinetic steps that may take place on heterogeneous surfaces. Other gases including oxygen and carbon monoxide have also been suggested to spillover. Furthermore, spillover has been shown to be involved in many different reactions including hydrogenation, dehydrogenation, partial and total oxidation, hydrocarbon isomerisation, hydrodenitrification, hydrodesulphurisation, gasification and hydrocarbon synthesis from syngas[25&28]

In 1940, Emmett[29] made one of the first observations of a spillover mechanism whilst investigating NH_3 synthesis and decomposition. He noticed that the rate of reaction increased as the particle size of the catalyst decreased, but only to a particular point, below which the rate did not increase any further. He concluded from this that a form of activated surface diffusion was taking place below a certain particle size of the metal catalyst.

Another early study specifically showing the action of *hydrogen* spillover was recorded in 1964 by Koobiar[30]. In this case, the presence of a Pt/Al_2O_3 (0.5 wt.% Pt) catalyst caused an instantaneous colour change from yellow to blue associated with the reduction of WO_3 to W_4O_{11} in H_2 gas which otherwise did not occur. He concluded that the H_2 had dissociated on the Pt catalyst even at room temperature and migrated to the WO_3, but acknowledged that the details of hydrogen migration were unknown.

Hydrogen spillover from a Pt catalyst on to a carbon support material was also investigated that same year[31]. The hydrogen was rapidly adsorbed by Pt and then migrated onto a carbon support with slow surface diffusion. The addition of 0.2 wt.% Pt to the carbon support resulted in a hydrogen uptake approximately four times higher than the pure carbon support as seen in Figure 2.1 below.

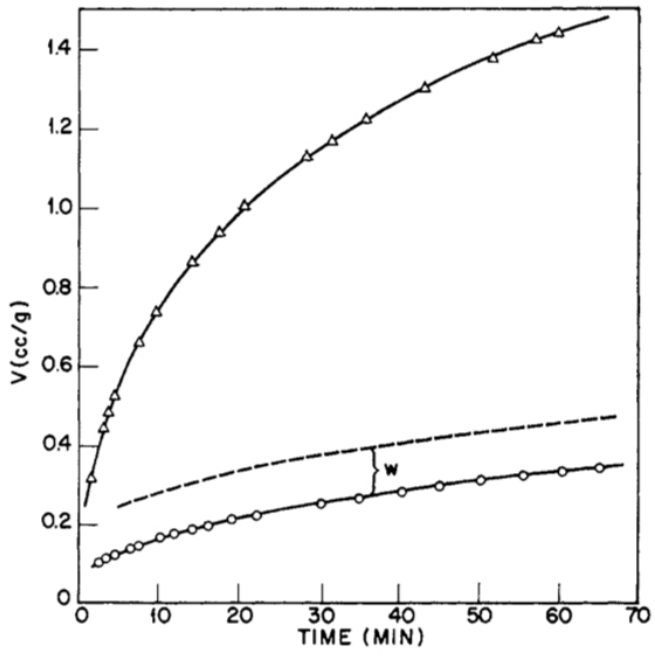

Figure 2.1 Spillover of hydrogen onto a carbon support. "Volume (STP cm^3/g) of hydrogen adsorbed as a function of time, at 350° and 60 cm.: O, Spheron 6; △, Spheron 6 + 0.2% Pt; w, adsorption of hydrogen corresponding to one hydrogen atom per platinum atom (calculated)" [31]

The phrase "spillover" was first coined to describe the mechanism observed in 1969 by Boudart et al.[32]. Later that year it was found[33] that the uptake of hydrogen by Pt/C was decreased significantly or nullified when the carbon on the Pt surface was burned off. They argued that this contamination by carbon was necessary to provide bridges that allowed surface diffusion of hydrogen from the Pt to the carbon support, as shown in Figure 2.2 below.

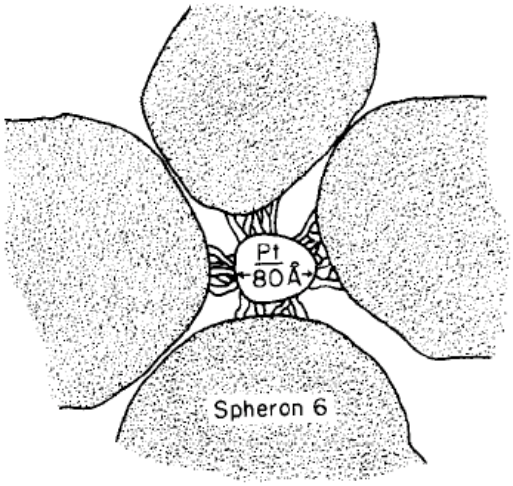

Figure 2.2 Illustrates carbon bridges between Pt and receptor. "Spillover of adsorbed atomic hydrogen from a platinum surface contaminated with carbon in the form of small particles and bridges to neighboring Spheron 6 particles"[33]

A similar study[34] to the first study in 1964[30] investigated the platinum catalysed reduction of WO_3 to H_xWO_3 at room temperature. They found that surface diffusion of hydrogen could be facilitated by the presence of a co-catalyst such as water or alcohol, which acted as a proton carrier. The higher the proton affinity of the co-catalyst was, the faster the rate of reduction. This suggests that the relationship between the receptor material and protons plays a key role in the diffusion of hydrogen.

2.2 – HYDROGEN SPILLOVER FOR STORAGE

Chen et al[35] reported a significant enhancement in hydrogen uptake for alkali-metal doped carbon nanotubes (CNTs). They measured that lithium and potassium doped CNTs adsorbed an extraordinary 20 wt.% and 14 wt.% of hydrogen respectively at ambient pressure and 473 - 673 K. Due to the potentially huge significance of this study, Yang[36] re-examined the results by repeating the same procedure, but the results were not repeatable. The effect of moisture in the hydrogen supply on hydrogen uptake of doped CNT was found to be the cause of the dramatic change in adsorption. This was attributed to the formation of alkaline hydroxides and hydrates. Yang used >99.999 % purity hydrogen from which "copious amounts of water were removed" using a series of traps. When this "dry" hydrogen was used for the measurements, 2.5 and 1.7 wt.% of hydrogen were adsorbed by Li and K doped CNTs respectively.

Hydrogen spillover was first used to describe the improvement in hydrogen storage materials by Leuking & Yang[37]. They found that the residual NiMgO catalyst used in the production of multi-walled carbon nanotubes (MWCNTs) also acted as a spillover source. Consequently these MWCNTs had a higher hydrogen uptake than those which had the catalyst completely removed by acid reflux. The interaction between metal and support was found to be crucial to the spillover mechanism as dry mixing of the MWCNT with catalyst did not enhance storage, but *in situ* production increased storage capacity by 40 %. Importantly it was also noted that the process was reversible at moderate temperatures giving a distinct advantage over metal hydrides and cryogenic porous materials. This reversibility also implied that spillover is reversible where the spiltover species diffuses back to the source of spillover. Yang and co workers have conducted much of the following literature on hydrogen spillover.[39,41,42,49,53]

2.2.1 Hydrogen spillover by physical mixing

The hydrogen uptake of physically mixed supported palladium and platinum catalysts with various carbons has been studied[38]. This was done at room temperature and included single wall carbon nanotubes (SWCNT), multiwall carbon nanotubes (MWCNT), graphitic nanofibres and activated carbon. The results showed that simple physical mixing of the catalyst with the carbon improved the overall uptake of hydrogen in all carbon materials tested. Interestingly, the baseline adsorption of the pure carbon was still the predominant factor in the size of the overall uptake.

This approach has also been used with porous Metal Organic Frameworks (MOFs) by Li & Yang[39]. They investigated the physical mixing (9:1 weight ratio) of MOF-5 or IRMOF-8 with a catalyst of 5 wt.% Pt on active carbon. They found that the hydrogen uptake was increased by a factor of 3.3 and 3.1 respectively at 298 K and 10 MPa. IRMOF-8 had the highest overall uptake of 1.8 wt.% at 298 K and 10 MPa. The adsorption was completely reversible and did not show any saturation up to 10 MPa.

2.2.2 Hydrogen spillover using carbon bridges

In a further study by Lachawiec et al.[40], bridge building was investigated by using carbon bridges. This was found to further increase the H_2 storage capacity of AX-21 by a factor of 2.9 at 298 K and 1 bar as seen in Figure 2.3.

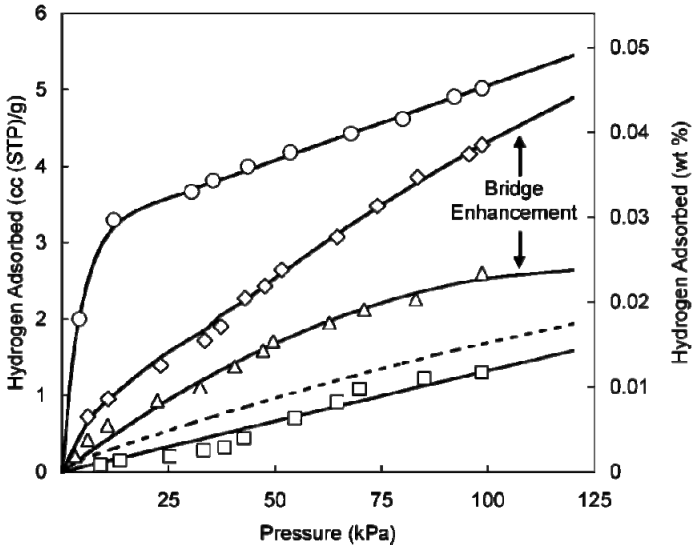

Figure 2.3 Bridging of carbon (AX-21) to palladium for increased hydrogen uptake. "Low-pressure hydrogen isotherms at 298 K for the AX-21 receptor: ○, 5 wt % Pd-C catalyst; ◇, AX-21/Pd-C/carbon bridge (8:1:1); △, AX-21/Pd-C physical mixture (9:1); □, AX-21. The dotted line is the sum of the fractional contributions based on uptake of individual mixture components"[40]

Using this method the receptor, catalyst and glucose (8:1:1 ratio) were mixed together. This mixture was then heated up to melt the glucose (to fill the gaps between catalyst and receptor) and then further heated to carbonise the glucose and form the carbon bridges as seen in Figure 2.3.

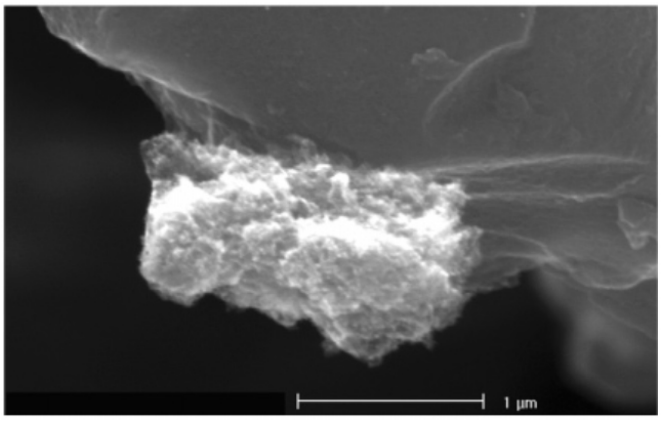

Figure 2.3 Pd particle connected to AX-21 via a carbon bridge[40]

Lachawiec et al.[40] also postulated that spillover was limited by surface diffusion on the

receptor rather than the dissociation of H_2 on the Pt catalyst. This implied that the contact and receptor properties are very important.

The possibility of improving the hydrogen spillover through carbon bridging on MOFs has also been investigated by Li & Yang[41]. They used a similar method to the previous study to bridge IRMOF 8. It differed because MOFs are thermally unstable at the temperatures needed for the carbonization of the glucose. Consequently a sucrose precursor was used instead, which has a lower melting and carbonization point to avoid collapse of the MOF structure. Complete carbonization of the bridges was confirmed by TGA. XRD and N_2 adsorption suggested that the structure of the MOF was still intact after the bridging process. The results showed spillover had a greater effect in MOFs than in carbons with improvements in hydrogen storage capacity from 0.5 % for pure IRMOF-8 to 2.2 – 4 wt.% for bridged IRMOF-8 at 298 K and 100 bar. However, there was also significant hydrogen uptake variation between the three bridged IRMOF-8 samples from 2.2 to 4 wt.% at 298 K and 10 MPa as shown in Figure 2.4.

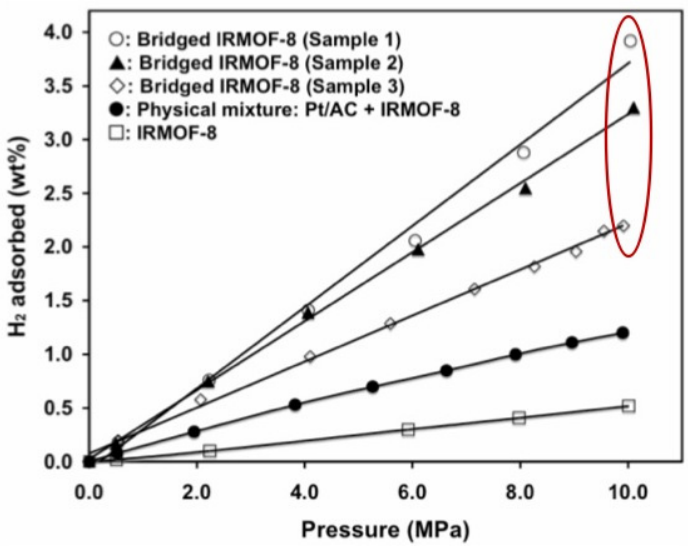

Figure 2.4 shows variable improvement in hydrogen uptake of bridged samples outlined in red[41]

This carbon bridging method has also been used to bridge MOFs with higher surface areas

such as MOF-177, which was found to enhance hydrogen adsorption by a factor of 2.5[42].

The problems with the physical mixing and bridging doping methods outlined above are the inherent inaccuracies associated with mixing, including sample amounts, grinding time and intensity which will in turn affect the quality of contact between catalyst, bridge and receptor particles. However, a recent study has used a mechanical means to produce a more repeatable method for bridging[43]. They investigated both mixed and bridged doping methods for two types of MOFs, MIL-101 and MIL-53. The difference in approach included mixing samples using a planetary ball miller under argon for 3hrs and using higher wt.% Pt/C catalyst. They found that physically mixed MIL-101 was improved by a factor of 2 and bridged MIL-101 by a factor of 3 at 5 MPa and 293 K.

An alternative method for doping giving more reproducible samples and better reliability can be achieved through chemical doping as discussed in the next section.

2.2.3 - Hydrogen spillover by chemical doping and other methods

Anson et al.[17] have doped both SWCNTs and Maxsorb with Pd by reacting the carbon support with a palladium organometallic complex $Pd_2(dba)_3 \cdot CHCl_3$ [tris(dibenzylidene-acetone)dipalladium(0)]. They carried out hydrogen uptake measurements at low and intermediate pressures as seen in Figure 2.5 below.

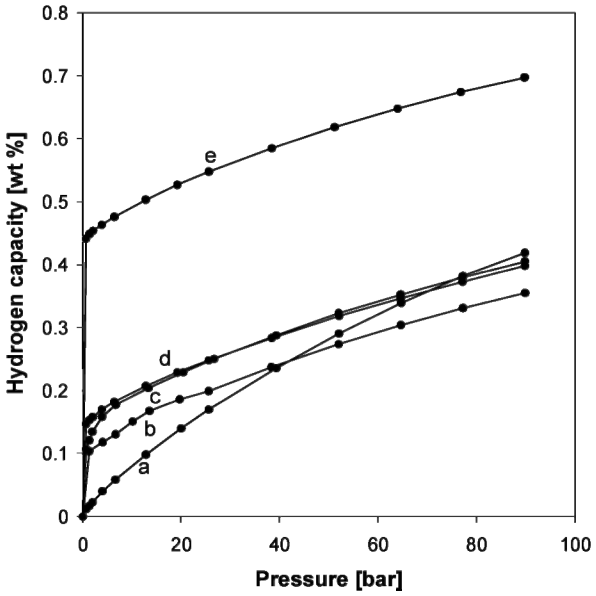

Figure 2.5 High pressure composition isotherm at room temperature for: (a) as received Maxsorb; (b) Maxsorb:Pd 1:1 second cycle; (c) Maxsorb:Pd 1:1 first cycle; (d) Maxsorb:Pd 1:2 second cycle; and (e) Maxsorb:Pd 1:2 first cycle[17]

The hydrogen adsorption characteristics differed from other work previously described for bridged samples by Li & Yang[41] with an initial rapid adsorption phase at low pressure followed by slower adsorption after the pressure had been raised by a few bar. At low pressures, the H/Pd atomic ratios in chemically doped palladium samples were higher than in bulk palladium. Anson et al. [17] suggested that this might be due to the spillover of hydrogen. However, at higher pressures and room temperature this effect of spillover was considered to be very low.

The ultrasound-assisted impregnation of H_2PtCl_6 into carbon has also been used to dope carbons[44]. The results showed enhancement by a factor of 2, to give 1.2 wt.% at 298 K and 10 MPa for a 5.6 wt % Pt doped AX-21 carbon. The adsorption of hydrogen was also completely reversible at 298 K. The US National Renewable Energy Laboratory and the US Department of Energy have also validated these results.

The chemical doping of MOFs by infiltrating Pd in to MOF-5 by using a palladium acetylacetonate precursor has also been investigated[45]. As with most studies of spillover the surface area was decreased significantly after infiltration, however hydrogen uptake still increased from 1.15 wt.% to 1.86 wt.% at 0.1MPa and 77 K.

The chemical doping method has also been compared with a plasma assisted reduction method on an activated carbon, Norit SX ULTRA[46]. Hydrogen storage at 298 K and 10 MPa was found to increase by a factor 3 by doping with 3 wt.% Pt using plasma assisted doping. The hydrogen uptake of the chemically doped sample was only enhanced by 54 % (under the same measurement conditions). This again suggests that the nature of contact between receptor and catalyst is a primary factor in the degree of spillover.

2.2.4 - Hydrogen spillover on other novel storage materials

Hydrogen spillover has also been shown on other novel materials, including; carbon templates using high surface area silicon and chemical vapour deposition[47]; templated carbons using a Na-Y zeolite template[48]; covalent organic frameworks[49]; and carbon foams[50]. Of particular note, the most recent study on carbon foams[50,51] has used a Pd/Hg catalyst, and reported an astonishing 8 wt.% H_2 uptake at 8 MPa and room temperature (see Figure 2.6 below). However these results are yet to be validated.

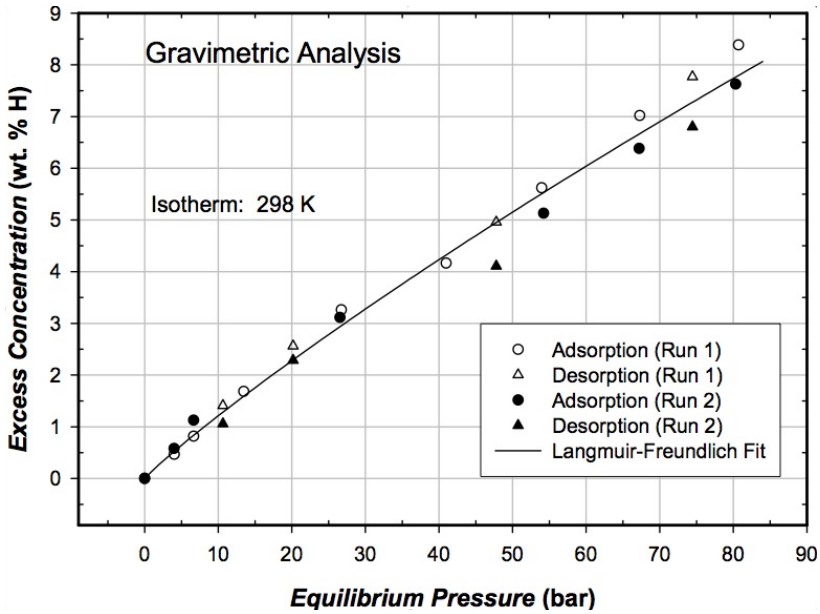

Figure 2.6 High pressure composition isotherm at room temperature for a Pd/Hg carbon foam[51]

2.3 - TEMPERATURE PROGRAMMED DESORPTION SUPPORT FOR HYDROGEN SPILLOVER

Bulk PdO (Sigma Aldrich) and Pd supported on activated carbon has been characterized using TEM, Temperature Programmed Desorption (TPD) and XRD[52]. The TPD of bulk Pd (see Figure 2.7) down to room temperature showed a single low temperature (~373 K) desorption peak whereas carbon supported Pd showed a slightly lower low temperature desorption peak and additional higher temperature (~873 K) desorption peak.

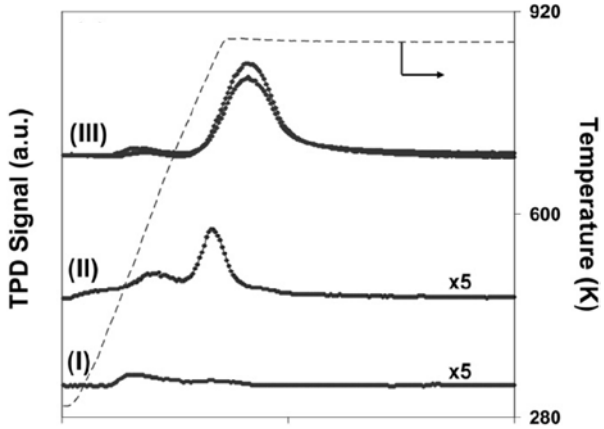

Figure 2.7 Hydrogen Temperature Programmed Desorption of bulk Pd (I), Physically mixed bulk Pd and Activated Carbon (II) and Pd chemically doped Activated Carbon (III)

These findings suggest that hydrogen associated with palladium and the support can be differentiated. Interestingly, the intensity of the second higher temperature peak was greater for the carbon supported Pd that had been chemically doped than the physical mixture of support and palladium. This was attributed to an enhanced palladium/support interface, which supports the idea that bridging the catalyst to the receptor would further enhance hydrogen spillover.

Sequential dosing of H_2 and D_2 on Pt/AX-21 and bridged IRMOF-8 has also been performed by Lachawiec and Yang[53]. The hydrogen desorption was then measured from the samples by TPD at several intervals. They found that desorption of the isotopes followed essentially the reverse doping sequence, suggesting that reverse spillover was taking place upon desorption.

2.4 – PRETREATMENT STUDIES

The formation of Pd-C phase has been observed by Ziemecki et al.[54] when Pd was heated in carbon containing gases such as ethylene, acetylene, or carbon monoxide. They concluded that a carbonaceous layer was deposited followed by the active diffusion of carbon through the Pd metal lattice. The addition of carbon to palladium results in the loss of ability to form β-PdH. The suppression of Pd hydride formation has also been observed with increasing Pd dispersion[55].

The effect of Pd precursor and pretreatment on the adsorption and absorption behavior of supported Pd catalysts has also been investigated by Krishnankutty et al.[56] They found that using a palladium acetylacetonate precursor contaminated the bulk and surface of the Pd crystallites in Pd/C catalysts during H_2 reduction at 573 K. This carbon could be removed by

calcination in oxygen. Further contamination also occurred during the following reduction-evacuation period at 573 K for Pd catalysts supported on a high surface area carbon black. They found that this could be prevented by chemisorbed layer of oxygen on the Pd surface. Figure 2.8 below shows some of the different circumstances that could occur in the case of Pd supported on carbon.

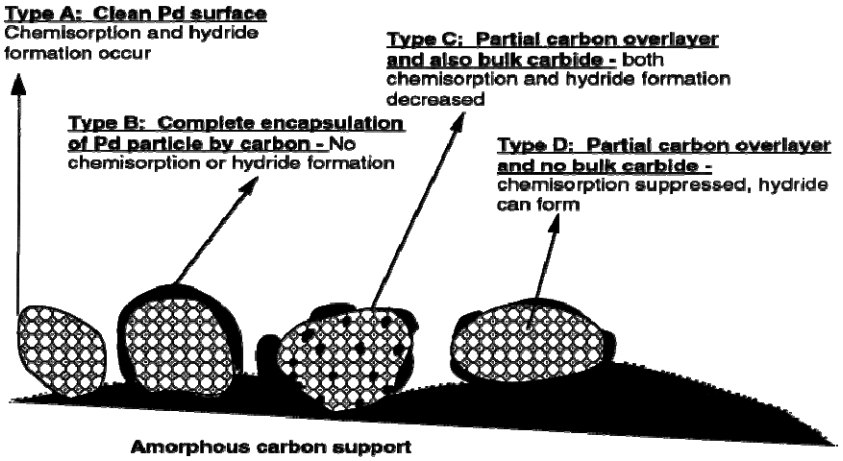

Figure 2.8 Carbon contamination of Pd particles supported on carbon[56]

Therefore, from the literature examined there seems to be a complex relationship between carbon and palladium. On one hand carbon bridging appears to improve uptake to a carbon support, whilst on the other, carbon contamination reduces the capacity of palladium to interact with hydrogen.

2.5 – SPILLOVER, SURFACE AREA & HEAT OF ADSORPTION

Normally, there is a strong correlation between surface area of materials and hydrogen uptake at 77 K. This is because the storage capacity is due to physisorption of H_2 molecules into the porous sites of the material. However at 298 K and 10 MPa, it has been suggested by Wang &

Yang[57] that the hydrogen uptake of bridged materials correlates much better with the heat of adsorption -ΔH (calculated from the Clausius-Clapeyron equation) as shown in Figure 2.10, rather than the BET surface area (Figure 2.9)

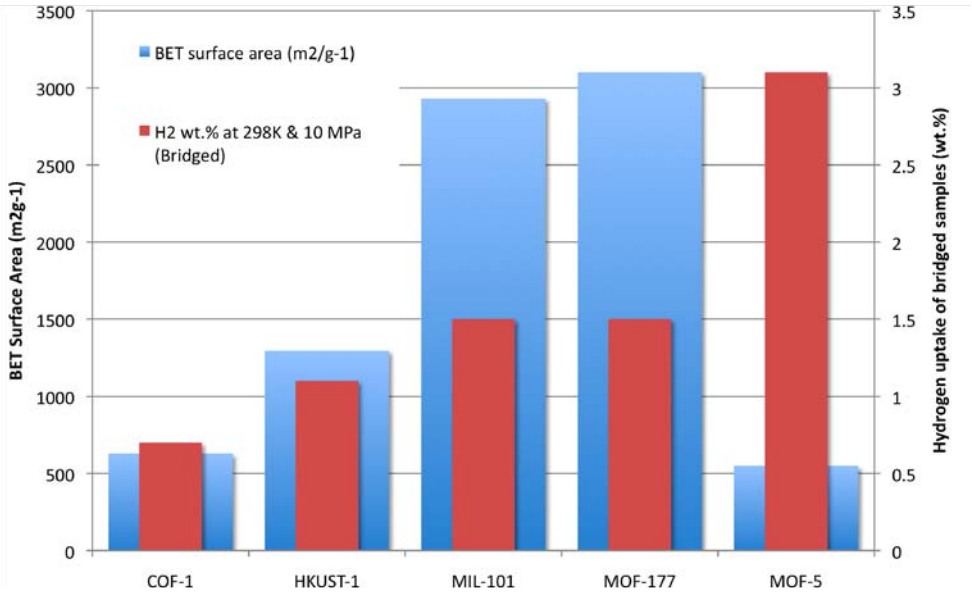

Figure 2.9 Relationship between surface area and H_2 uptake for bridged porous materials at room temperature[57]

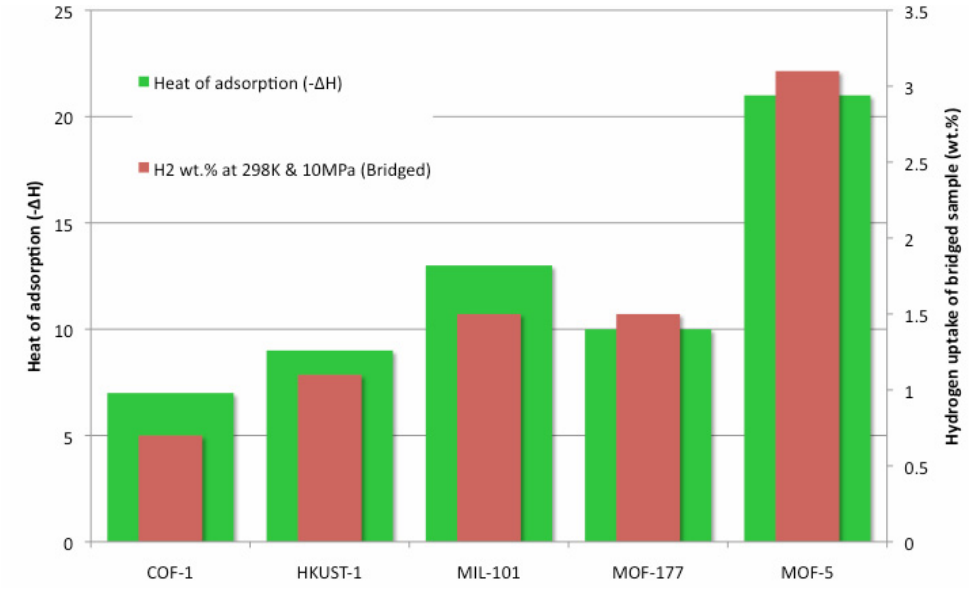

Figure 2.10 Relationship between heat of adsorption and H_2 uptake for bridged porous materials at room temperature[57]

Wang & Yang[57] propose that the heat of adsorption is related to metal content. This is most clearly seen when comparing MOF-177 with IRMOF-8. These both have the same type of metal clusters, ZnO_4, but the metal content of IRMOF-8 is higher than MOF-177 due to the smaller pore sizes. This results in a higher H_2 uptake by bridged IRMOF-8 despite bridged MOF-177 having a significantly higher surface area of 3100 m^2/g compared with 548 m^2/g.

The rate of spillover has been proposed to be dependent on the rate of adsorption by the catalyst and also the rate of surface diffusion away from the source. Surface diffusion of hydrogen has been proposed to be the rate limiting step in the spillover process[31].

2.6 – SUMMARY OF SPILLOVER ENHANCEMENTS

Table 2.1 below shows a summary of some of the receptor materials and catalysts that have been investigated for hydrogen spillover at ambient temperature and the associated enhancement in hydrogen uptake.

Table 2.1 "Spillover" hydrogen uptake enhancements for a wide range of doped carbon and MOF receptors (* Measurement to be verified)

Author & conditions	Receptor & BET* surface area	Uptake without dopant	Catalyst	Doping method	Uptake with dopant	Enhancement
Robell et al., 1964[31]	Spheron 6 100 m^2/g	0.35 cm^3/g	0.2 wt.% Pt	-	1.4 cm^3/g	4
Yang, 1999[36]	MWCNT 148 m^2/g	0.4 wt.%, 1 atm (Chen 1999)	Li, atomic ratio 1:15	Chemical	2.5 wt.%	6.25
			K, atomic ratio 1:15	Chemical	1.82 wt.%	4.55
Lueking& Yang, 2001[37]	MWCNT	Below detection	NiMgO	Chemical	0.58 - 0.65 wt.% 298 K, 1 bar	Significant
Lueking& Yang, 2004[38]	Carbon nanotubes	-	Pd	Physical mixing	-	3
Zielinski, 2005[58]	Activated Carbon	0.1 wt%, 293 K, 30 bar	1wt.% Ni	Chemical	0.53 wt.%, 293 K, 30 bar	5.3
Zacharia, 2005[59]	Carbon nanotubes	0.53 wt% 298 K 2 MPa	V	Chemical	0.69 wt.% 298 K 2 MPa	~0.3
			Pd	Chemical	0.66 wt.% 298 K 2 MPa	~0.3

Lachawiec et al., 2005[40]	SWNT		10 wt.% Pd/C	Bridged	1.6 wt.% 298 K, 100 kPa	1.6
	AX-21	*0.6 wt% 298 K, 10 MPa*	10 wt.% Pd/C	Physical mixing	0.85 wt.%, 298 K, 10 MPa	1.42
	AX-21	*0.6wt% 298K, 10 MPa*	10 wt.% Pd/C	Bridged	1.8 wt.%, 298 K, 10 MPa	3
Li & Yang, 2006[41]	IRMOF-8	0.5 wt.% 298 K, 10 MPa	10 wt.% Pt/AC	Bridged	2.2 – 4 wt.% 298 K, 10 MPa	6.2 (Avg.)
Anson et al., 2006[17]	Carbon nanotubes	0.21 wt.% 298 K 9 MPa	13-31 wt.% Pd 5-7 nm	Chemical	0.51 wt.% 298 K 9 MPa	2.43
	Maxsorb activated carbon	0.42 wt.% 298 K 9 MPa	30-50wt.% Pd 32-42 nm	Chemical	0.7 wt.% 298 K 9 MPa	0.69
Li & Yang, 2007[60]	AX-21	0.6 wt% 298 K, 10 MPa	5.6 wt.% Pt, 2nm	Chemical	1.2 wt.%, 298 K, 10 MPa	2
Li & Yang, 2007[42]	MOF-177	0.62 wt.% 298 K, 10 MPa	5 wt.% Pt/AC	Bridged	1.5 wt.% 298 K, 10 MPa	2.5
Li & Yang, 2007[46]	Activated Carbon 1200 m^2/g	~0.3 wt.% 298 K, 10 MPa	3 wt.% Pt	Chemical	~0.5wt.%298 K, 10 MPa	0.54
				Plasma assisted doping	~0.9 wt.% 298 K, 10 MPa	~3
Liu et al., 2007[43]	MIL-101 2578 m^2/g	0.37 wt.% 293 K, 5 MPa	20 wt.% Pt/C	Physical mixing	0.75 wt.% 293 K, 5 MPa	2
			20 wt.% Pt/C	Bridged	1.14 wt.% 293 K, 5 MPa	3
	MIL-53 299 m^2/g (Langmuir)	No obvious hydrogen adsorption	20 wt.% Pt/C	Physical mixing	0.43 wt.% 293 K, 5 MPa	Significant
			20 wt.% Pt/C	Bridged	0.63 wt.% 293 K, 5 MPa	Significant
Sabo et al., 2007[45]	MOF-5 2885 m^2/g (specific SA)	1.15 wt.% at 1 atm, 77 K	1 wt.% Pd	Chemical	1.86 wt.% 1 Atm, 77 K	1.62
Campesi et al., 2008[47]	Carbon Template 847 m^2/g TSA	0.01 wt.%, 298 K, 0.5 MPa	10 wt.% Pd	Chemical	0.08, 0.06 &0.053 wt.%, 298 K, 0.5 MPa	5.3 - 8
Lachaweic& Yang, 2008[53]	Templated Carbon 3400 m^2/g	0.8 wt.%, 298 K, 10 MPa	6 wt.% Pt	Chemical	1.35 wt.%, 298 K, 10 MPa	1.7
Li & Yang, 2008[49]	COF-1 628 m^2/g	0.26 wt.% 298 K, 10 MPa	5 wt.% Pt/AC	Bridged	0.68 wt.% 298 K, 10 MPa	2.6
	HKUST 1296 m^2/g	0.35 wt.% 298 K, 10 MPa	5 wt.% Pt/AC	Bridged	1.12wt.% 298K, 10 MPa	3.2
	MIL-101 2931 m^2/g	0.51 wt.%, 298 K, 10 MPa	5 wt.% Pt/AC	Bridged	1.43wt.% 298K, 10 MPa	2.8
Bourlinos et al. 2008[50]	Carbon Foam	Negligible	10 wt.% Pd	-	2.1 wt.%, 298 K, 3 bar*	Significant
Bourlinos et al. 2008[50]	Carbon Foam	Negligible	Pd/Hg	-	8 wt.%, 298 K, 8 MPa*	Significant

2.7 – BIOSYNTHESIS OF PALLADIUM NANOPARTICLES

Normally small particles of palladium are produced by purely chemical means by the precipitation of the solid phase from a palladium solution, which involves the nucleation and particle growth of palladium particles. A novel and potentially more sustainable alternative is

to manufacture palladium nanoparticles for catalysis through biosynthesis. This process takes advantage of bacteria, which use enzymes to deposit metal ions from solution to the cell surface layers as a detoxification mechanism (see Figure 2.11). This is a relatively rapid and inexpensive method in comparison.

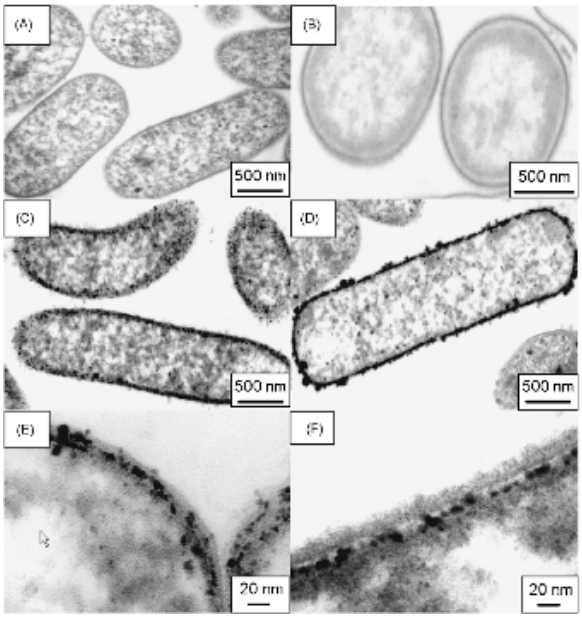

Figure 2.11 TEM of Pd nanoparticles in the cell walls of bacteria[61]

If the bacteria containing palladium could be pyrolysed, the resulting carbon could then potentially be used, if it had a sufficiently high surface area, as a support for the nanoparticles of palladium already present. Therefore creating a hydrogen storage material with catalyst from one process.

This project will briefly investigate biologically produced palladium nanoparticles from waste material, which were produced by Mikheenko & Macaskie in Biosciences[62]. This mechanism of biosyntheis has already been used to recover other precious metals, although only certain types of bacteria are capable of the biosynthetic process. Bacteria that have been used to reduce Na_2PdCl_4 (sodium tetrachloropalladate (II)) to palladium nanoparticles include various

species of Desulfovibro, namely desulfuricans, fructosivorans and vulgaris[63] Shewanella oneidensis[64] and Bacillus Sphaericus[61]. The biosynthetic process also reduces waste products and pollution by removing unnecessary chemical reagents used in chemical production methods.

The catalytic activity of the biosynthesized Pd has been further investigated (see Figure 2.12) for potential use in fuel cells by comparing it to commercial 5 % Pd-graphite catalysts by Creamer et al.[61] They found that the initial rates of reaction were up to 92 % of that of the commercial catalyst.

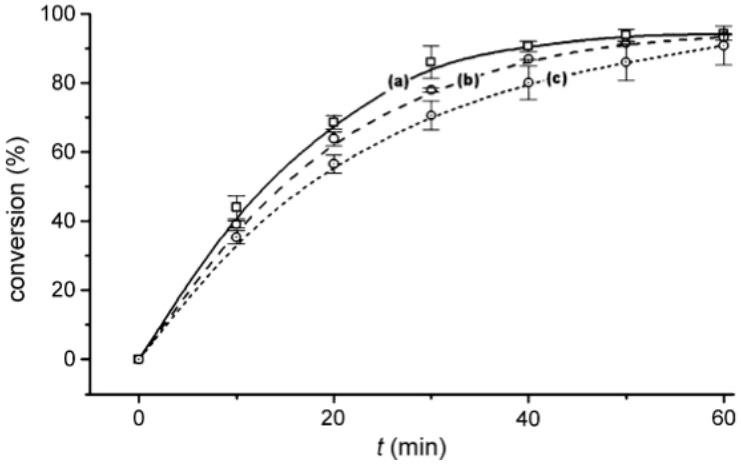

Figure 2.12 Comparison of the conversion rates of itaconic acid by: a) 5% Pd on graphite (Johnson–Matthey); b) 2% Pd on B. sphaericus; and c) 5% Pd on D. desulfuricans.[61]

It has also been found[64] that the particle size of palladium produced can be varied by altering the ratio of palladium to cell dry weight (Pd:CDW). Consequently the catalytic reactivity of palladium produced could potentially be controlled to give properties on demand. It was found that at high Pd:CDW ratios the particles were larger and at low Pd:CDW ratios the particles were smaller.

2.8 - AIM

Therefore, the primary aim of this research project is to investigate whether a "spillover" effect, leading to enhanced hydrogen uptake, can be achieved in three types of high surface area materials at room temperature: a carbon furnace black (Black Pearls 2000); an activated carbon (Maxsorb); and a metal organic framework compound (MOF-5). Particles of palladium will be deposited onto the surface of these materials through bridging and chemical doping techniques. The physical characteristics and hydrogen storage properties of these materials will then be measured. In addition, the hydrogen storage properties of a biopalladium/carbon material, produced in the School of Biosciences (University of Birmingham), will be very briefly investigated.

3 - EXPERIMENTAL APPROACH

3.1 MATERIAL SYNTHESIS

3.1.1 As-received samples

Samples of Maxsorb (activated carbon), Black Pearls 2000 (carbon furnace black) and MOF 5 (Metal Organic Framework) were obtained from Nottingham University, Cabot Corporation and BASF, respectively. These as-received samples were compared with those bridged and chemically doped with palladium.

3.1.2 Bridged samples

All three materials were bridged by glucose or sucrose obtained from Sigma Aldrich using a similar method to that given in the literature[40 41] to try to improve the contact between the Pd catalyst and receptor by creating carbon bridges between them. The ratios of receptor, catalyst and bridge material are shown in the table below.

Receptor	Catalyst	Bridge material
200 mg MOF-5	25 mg 5 wt.% Pd on Activated Carbon	33.2 mg Sucrose
200 mg Black Pearls	20 mg 5 wt.% Pd on Activated Carbon	20 mg Glucose
200 mg Maxsorb	20 mg 5wt.% Pd on Activated Carbon	20 mg Glucose

Table 3.1 Composition of bridged materials

The carbon bridged samples were mixed in air using an agate mortar and pestle for 30 minutes and then heated under argon at 1 K/min to 453 K and held for 3 hrs to melt the bridge material. They were then further heated to 673 K at 1 K/min for 6 hrs to carbonise the glucose

bridge material. A similar method was used for MOF-5. The bridged samples were mixed in air using an agate mortar and pestle for 1 hr and then heated under argon at 1 K/min to 473 K and held for 3 hrs to melt the bridge material. They were then further heated to 523 K at 1 K/min for 12 hrs to carbonise the sucrose bridge material. Sucrose has a lower carbonisation point (523 K) and was used as the bridge material because the temperatures required for the carbonisation of glucose (673 K) would damage the structure of MOF-5. The bridged MOF-5 samples were then stored in an inert atmosphere to await testing.

3.1.3 Chemically doped samples

A chemical Pd-doping method was also used by Johnson Matthey to deposit 6 wt.% palladium onto the Black Pearls sample using a solution-based technique which is commonly used for depositing Pd onto fuel cell membranes. Further details could not be provided, as this technique is confidential.

3.2 MATERIAL CHARACTERIZATION

The hydrogen storage characteristics (kinetics and pressure composition isotherms) of all the materials were measured gravimetrically or volumetrically using a Hiden Pressure controlled thermogravimetric balance (IGA) or a Hiden Sieverts apparatus (HTP). These different instruments were used firstly because this enabled measurements to be made over different pressure ranges, and secondly, to try to eliminate errors specific to one particular type of instrument. The purity of hydrogen used in both techniques was 99.99996 %, which was also passed through a liquid nitrogen trap. The purity of helium used for the mass spectrometry and in the pycnometer was 99.99995%.

3.2.1 Gravimetric Hydrogen Measurements

A Hiden Intelligent Gravimetric Analyser (IGA) was used to monitor the mass change of samples verses time at specific temperatures and pressures (see Figure 3.1). This technique requires buoyancy correction due to the sample and counterweight displacing different volumes of gas and sometimes being at different temperatures.

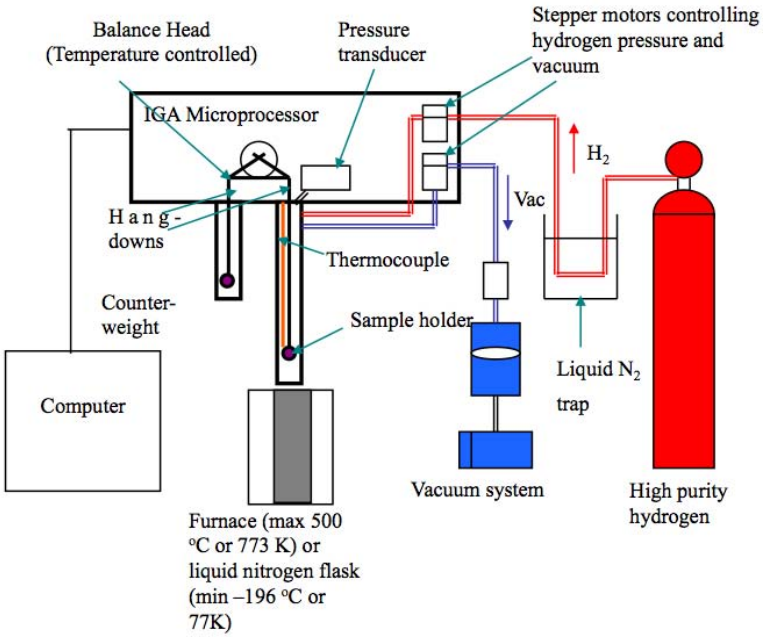

Figure 3.1 Schematic diagram of the Hiden Intelligent Gravimetric Analyser (IGA) system[14]

All samples (~100 mg) were loaded in air and then outgassed using a combination of membrane and turbomolecular pumps to about 10^{-5} mbar. The temperature was then increased to 673 K for carbons and 523 K for MOF-5 to remove any moisture or solvents that may remain from the sample synthesis. These conditions were maintained until the mass of the sample had stabilised. The sample was then cooled back to room temperature and the dry mass was recorded in the vacuum. Measurements to produce a pressure composition isotherm

were then performed, which consists of a series of pressure steps at room temperature. At each pressure step the mass change was monitored against time and allowed to reach equilibrium before moving onto the next pressure step. After all pressure steps were completed, uptake was plotted against pressure. The buoyancy of the sample at each pressure step was calculated within the software by using the Archimedes principle for the upthrust of an object. The weight change due to buoyancy Δ_{wb}, of an object of density ρ_s and mass m_s, in a gas of density ρ_g can be given as:

$$\Delta w^{b} = \Delta v \rho_g g = \frac{m_s \rho_g g}{\rho_s}$$

where Δv is the volume of gas displaced by the object and g is the acceleration due to gravity. After each run was completed on the IGA, the sample bucket was carefully washed with industrial methylated solvent in an ultrasonic bath and dried before loading the subsequent sample.

BET (Brunauer, Emmett and Teller) surface area measurements were also carried out to calculate the surface area of selected samples. The reactor was immersed in a dewar of liquid nitrogen to reach 77 K, in order to cool the sample. At this low temperature nitrogen gas may liquefy in the pores and on the surface of the sample. The quantity of gas adsorbed can be correlated to surface area.

3.2.2 Volumetric Hydrogen Measurements

A Sieverts volumetric technique (Hiden HTP) was also used to measure hydrogen uptake (see Figure 3.2). The HTP measures a pressure drop via a pressure transducer in a sealed volume

(5 cm^3). The apparatus is comprised of two volumes (dosing and sample volume). During the experiment the dosing volume is filled to a programmed pressure and allowed to equilibrate. The valve between the dosing and sample volumes is then opened at which point the pressure falls by approximately half due to the overall larger volume. If the sample in the sample volume absorbs hydrogen then the pressure will continue to fall and eventually reach equilibrium. As the pressure, temperature, sample mass and volume of the system are known, it is possible to calculate an amount of gas absorbed and subsequently a wt.% of hydrogen absorbed. For desorption a pressure rise will be observed. The calibration of the sample volume required the input of 9 bar pressure, 5 times per calibration and this was repeated at least three times. The sample volume was then outgassed using a turbomolecular pump. Due to the low density and fine particle size of many of the samples, glass beads and ceramic wool were required to prevent the sample from being propelled out of the sample volume into the rest of the machine.

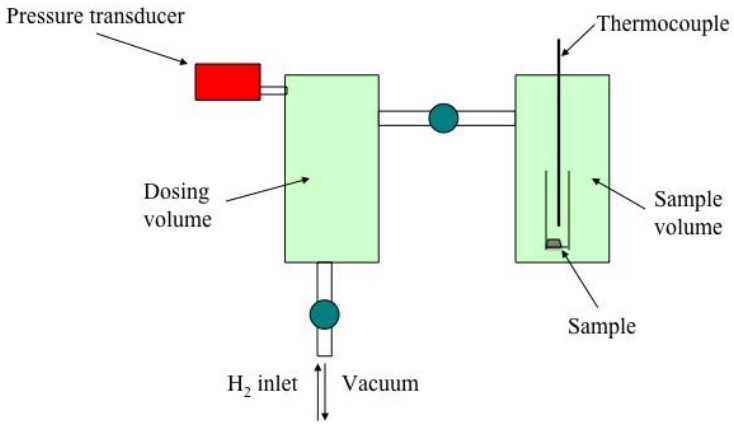

Figure 3.2 Schematic diagram of Hiden HTP system

After each run the sample volume was carefully washed with industrial methylated solvent in an ultrasonic bath and dried before loading the subsequent sample.

3.2.3 Temperature Programmed Desorption (TPD)

Mass spectrometry and TPD were also used in conjunction with HTP to measure the temperature dependence of hydrogen desorption from the samples. The samples were first hydrided at room temperature for 6 hrs and 100 bar to saturate the sample. The samples were consequently cooled to 79 K using a liquid nitrogen cryostat and slowly heated up to 773 K at a ramp rate of 5 K/min in a flow of helium (purity 99.9999995 %) at 5 cm^3/min.

3.2.4 X-ray Diffraction (XRD)

Powder XRD was performed on a Bruker D8 Advance machine and was used to verify the composition and particle size of the palladium. This uses an X-ray source, sample stage and a detector as shown in Figure 3.3. A beam of electrons are produced by heating a tungsten filament, which are then accelerated using a target copper anode. These electrons cause ionisation and the production of Cu K α and β radiation. The X-rays are then filtered using a metal foil or a crystal monochromator to produce a monochromatic source of X-rays. When these X-rays are incident on the sample they are diffracted by the atomic structure of the sample. The resulting diffraction pattern of the X-rays at certain angles are then interpreted using Bragg's Law to show structural information about the sample as shown below.

$$n\lambda = 2d \cdot sin\theta$$

n - an integer determined by the order given

λ - wavelength of x-rays, and moving electrons, protons and neutrons

d - spacing between the planes in the atomic lattice

θ - angle between the incident ray and the scattering planes

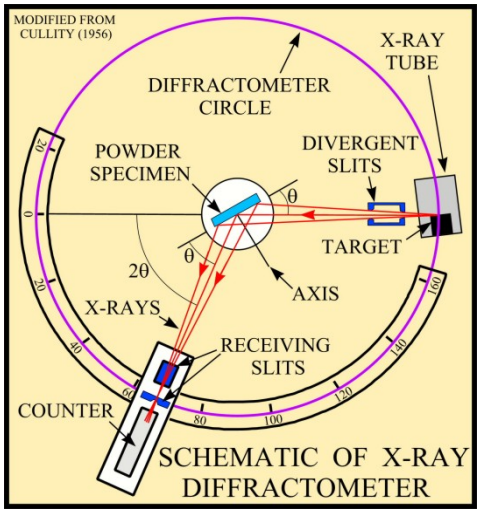

Figure 3.3 schematic of an X-ray diffraction machine in reflection mode[65]

The Scherrer equation as shown below was then applied to the XRD data to calculate crystallite size.

$$\beta_{hkl} = \frac{K\lambda}{L_{hkl}\cos\theta_{hkl}}$$

β - width of peak at half maximum intensity of a specific phase ($_{hkl}$) in radians

K - constant according to method used to calculate breadth

λ - wavelength of incident x rays

L - crystallite length

θ - centre angle of the peak

3.2.5 Gas Pycnometry

A Micromeritics AccuPyc 1340 gas pycnometer (Figure 3.4) was used within an Ar glovebox to measure the skeletal density of the samples. The sample container was 2/3 filled with a sample and the weight was recorded on a mass balance (normally ~100 mg). The pycnometer with sample was purged 30 times with helium to remove impurities. It uses a similar technique to the HTP with a reference and sample volume. The sample volume was pressurised to 19.5 Psig (1.35 bar) at 0.01 Psig/min (0.7 mbar/min) and the valve between the sample volume and reference volume was then opened. Using the pressure change between the sample and reference volumes, the sample density was then calculated. This process was repeated for 50 cycles to obtain a reliable result.

Figure 3.4 Photograph of a Micromeritics AccuPyc 1340 gas pycnometer[66]

3.3 EXPERIMENTAL ERRORS

The hydrogen storage capacities of high surface area materials at room temperatures are low, typically ~0.1 wt% from this work. Consequently, errors potentially have a larger impact on

the overall uptake. Errors were minimized by the use of both gravimetric and volumetric hydrogen measurements. Inaccuracies and errors associated with the IGA measurement used may have included;

- Small buoyancy correction errors caused by inaccurate density measurements.
- Impurities such as water in the gas stream adsorbing on carbon are shown by drift and taking a very long time for the mass to reach equilibrium (Figure 3.5). This effect was minimized by the use of liquid nitrogen traps.

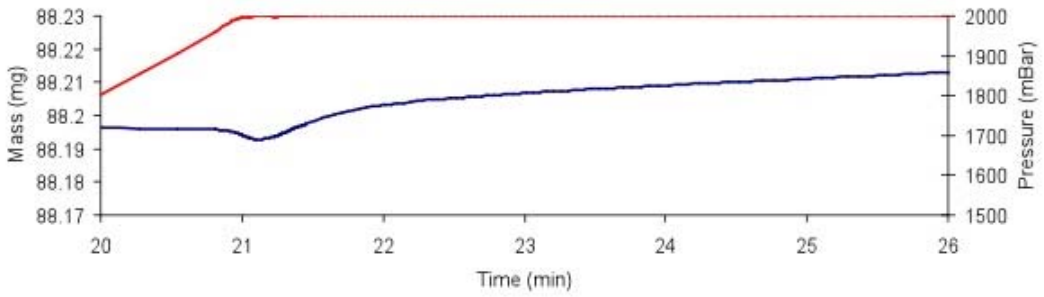

Figure 3.5 Model pressure composition isotherm shows apparent uptake (blue line) whilst pressure remains constant (red line)

Inaccuracies and errors associated with the Hiden HTP measurement on Bridged Maxsorb may have included;

- Temperature gradient correction between variable sample volume and dosing volume
- Correction for sample volume and density, potential for volume expansion of sample
- Errors from switching between different gases
- Leaks on pycnometer resulting in density errors

- Gas leaks, which are often difficult to distinguish between uptake (Figure 3.6)

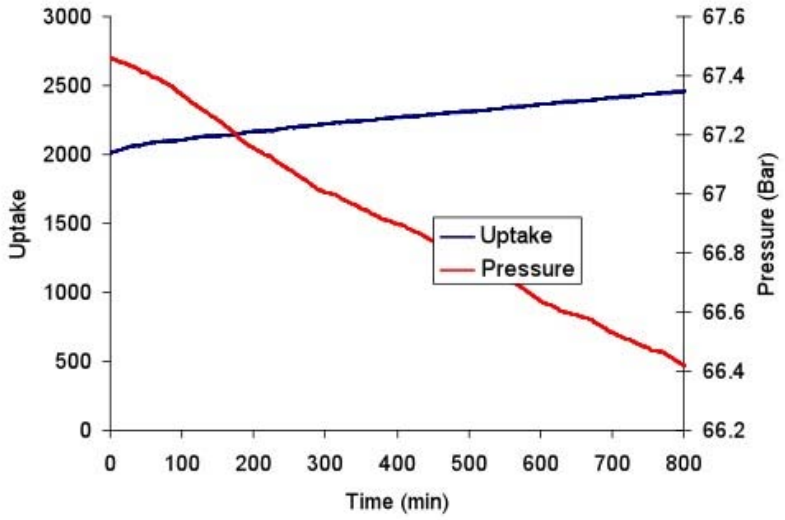

Figure 3.6 Pressure composition isotherm shows apparent uptake of an empty sample container caused by a leak

The volumetric system does have the advantage over the gravimetric system in that higher pressures can be achieved and it does not have to compensate for buoyancy effects. This means that although both techniques suffer from errors, they are of a different nature. The errors were further minimized by the following;

- Using high purity hydrogen (99.99995 %) and helium (99.99995 %)
- Using liquid nitrogen to scrub the inlet gas
- Using fittings and regulators suitable for high purity gas.
- Monitoring the kinetic points during the pressure composition isotherm to ensure that each point reached equilibrium before going on to the next point.

4 - RESULTS & DISCUSSION

Table 4.1 below summarises the synthesised materials and their characterisation.

Material	Treatment	Wt.% Pd	Characterisation
Palladium powder	-	100	XRD, TPD, HTP
Pd/C (Sigma Aldrich)	-	5	XRD
Maxsorb (Activated carbon)	As received	-	IGA
	Pd/C bridged	0.44*	XRD, IGA, HTP
Black Pearls 2000 (Carbon furnace black)	As received	-	IGA
	Pd/C bridged	0.44*	XRD, IGA
	Johnson Matthey Chemically doped	6	XRD, IGA, TPD
MOF-5 (Metal Organic Framework)	As received	-	XRD, IGA
	Pd/C bridged	0.44*	XRD, IGA

Table 4.1 Summary of materials, treatment and characterisation

XRD – X-ray Diffraction

IGA – Hydrogen sorption measured on a Hiden IGA gravimetric system

HTP – Hydrogen sorption measured on a Hiden HTP volumetric system

TPD – Temperature Programmed desorption

* 0.44 wt.% was calculated as follows

5 wt.% of Pd in 20 mg Pd/C = 1 mg of Pd

= 19 mg of Carbon

Receptor material = 200 mg

Bridge material (assuming fully carbonised) = 8 mg of Carbon

1 mg of Pd/Total mass of 228 mg x 100 = 0.44 wt.% Pd

4.1 XRD OF MATERIALS

4.1.1 XRD of commercial activated carbon supports doped with palladium

XRD was carried out on commercial activated carbon supports (Sigma Aldrich) doped with 1 wt.% (black), 3 wt.% (red), 5 wt.% (blue), 10 wt.% (green), 30 wt.% (pink) of palladium as seen Figure 4.1 below.

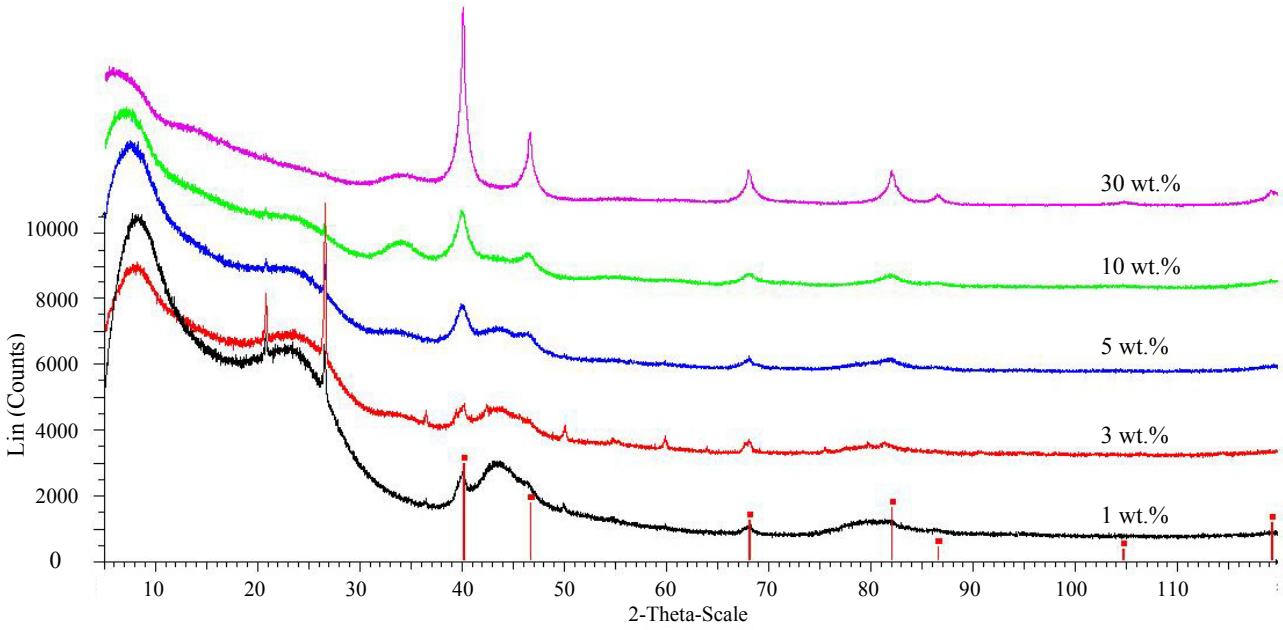

Figure 4.1 XRD data of 1, 3, 5, 10 & 30 wt.% Pd on activated carbon from Sigma Aldrich. The red vertical lines signify Pd (00-046-1043 PDF database)

The peak angles displayed were consistent with as-received Pd of cubic symmetry as shown by the vertical red lines on the x axis. The Pd peaks became progressively smaller as the weight percentage of Pd was decreased. The 1% Pd on activated carbon trace (black) showed especially small peaks. This suggested that it would be difficult to distinguish Pd deposited on

the doped receptor materials because they also contained very low percentages of palladium (around 0.44 wt%). The peaks at 20°, 27°, 50° and 60° for 1 & 3 wt.% Pd activated carbon samples were unassigned. They may have been due to contamination of the substrate material that was used to contain the sample for XRD. However, these peaks were not considered significant because these samples were not being used to bridge receptor materials, only the 5 wt.% Pd on carbon (blue line). The particle size of palladium from this 5 wt.% Pd on carbon was unable to be calculated from the full width half maximum values due to the small and undefined peaks.

Bridged materials consisted of the receptor (either carbon or MOF), 5 wt.% Pd/C activated carbon and a sugar (carbonised), which was used to bind them together (8:1:1 ratio). The final overall wt.% of palladium used in the bridged materials was around 0.44 wt.%. These proportions were chosen as it has been reported that hydrogen uptake can be enhanced by approximately a factor of three for carbons[38] and MOFs[41].

4.1.2 XRD of Bridged Black Pearls 2000

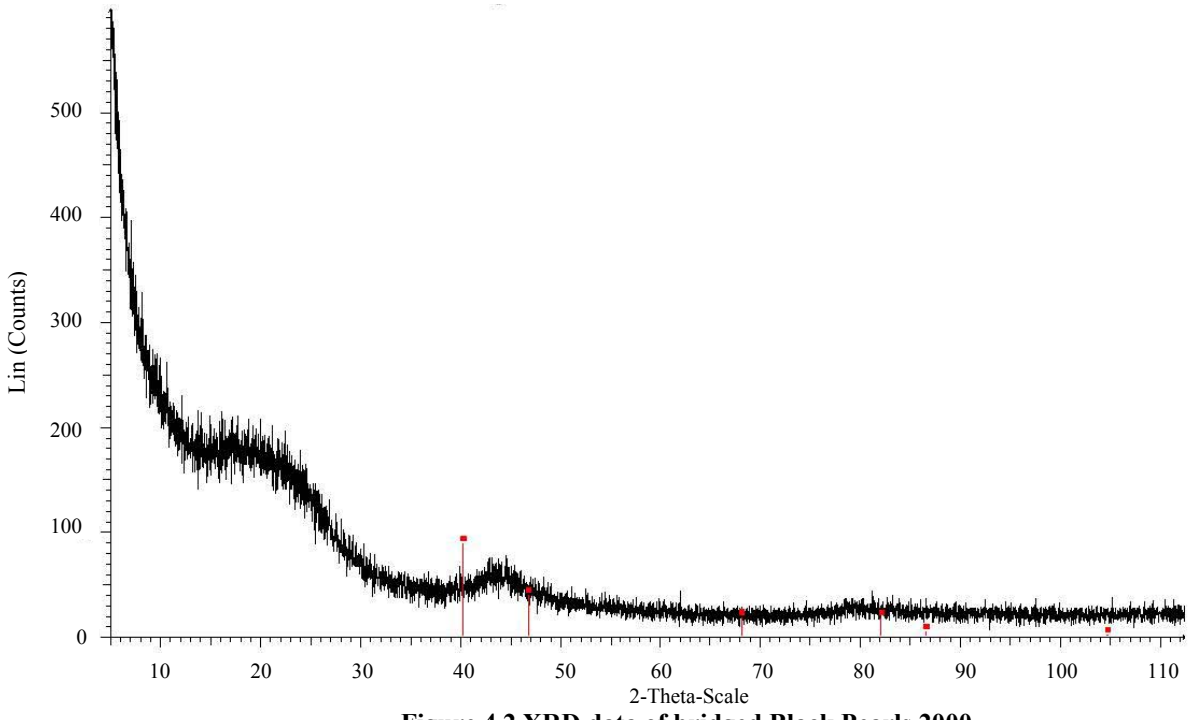

Figure 4.2 XRD data of bridged Black Pearls 2000

The bridged Black Pearls sample did not show any XRD peaks associated with Pd (see Figure 4.2). This was attributed to the very low wt.% of palladium deposited (0.44 wt.%); this value was selected in order to match that used in the literature[38]. It was not possible to calculate the Pd particle size from the full width half maximum due to the lack of peaks. However, it seems unlikely that the Pd grain/particle size would have changed from the starting material through the bridging process.

4.1.3 XRD of 6 wt.% Black Pearls 2000 (Johnson Matthey)

Separate XRD data was provided by Johnson Matthey on the chemically doped 6 % Pd Black Pearls carbon sample (black line). This was then compared to as-received Black Pearl (blue line) as seen in Figure 4.3 below.

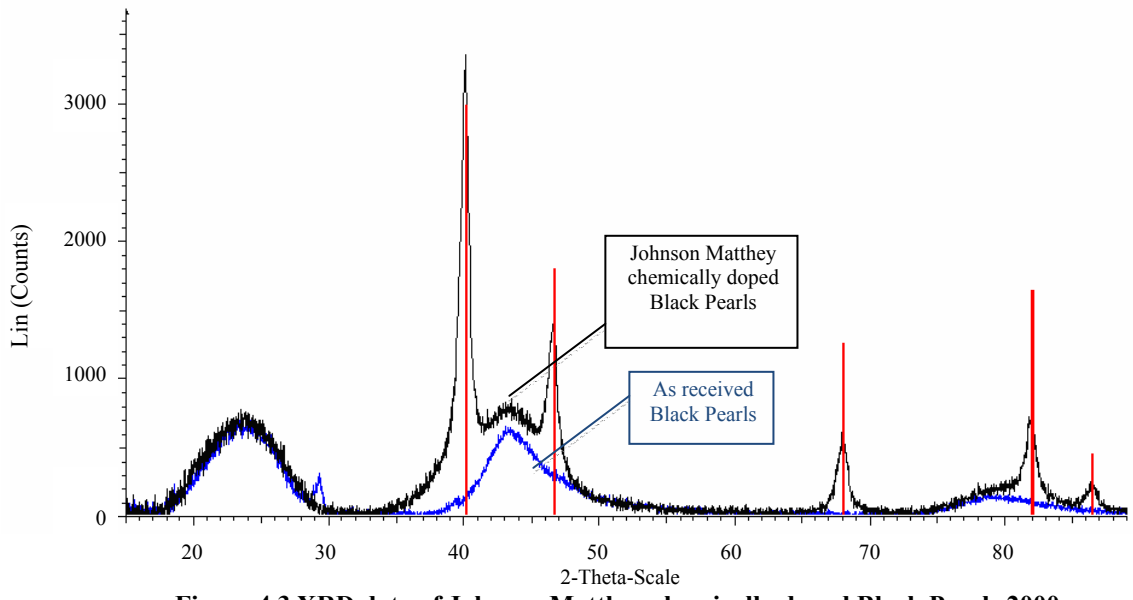

Figure 4.3 XRD data of Johnson Matthey chemically doped Black Pearls 2000

Johnson Matthey analysis of the XRD diffraction pattern showed that the chemically doped Black Pearls was composed of a significant amount of palladium supported on carbon. A palladium crystallite size of 12.2 nm was calculated using the Scherrer equation, and the peaks were found to be consistent with Pd of cubic symmetry. The peaks had significantly higher intensities than those of the bridged samples, which was due to the much higher 6 wt.% Pd used.

4.1.4 XRD of Bridged Maxsorb

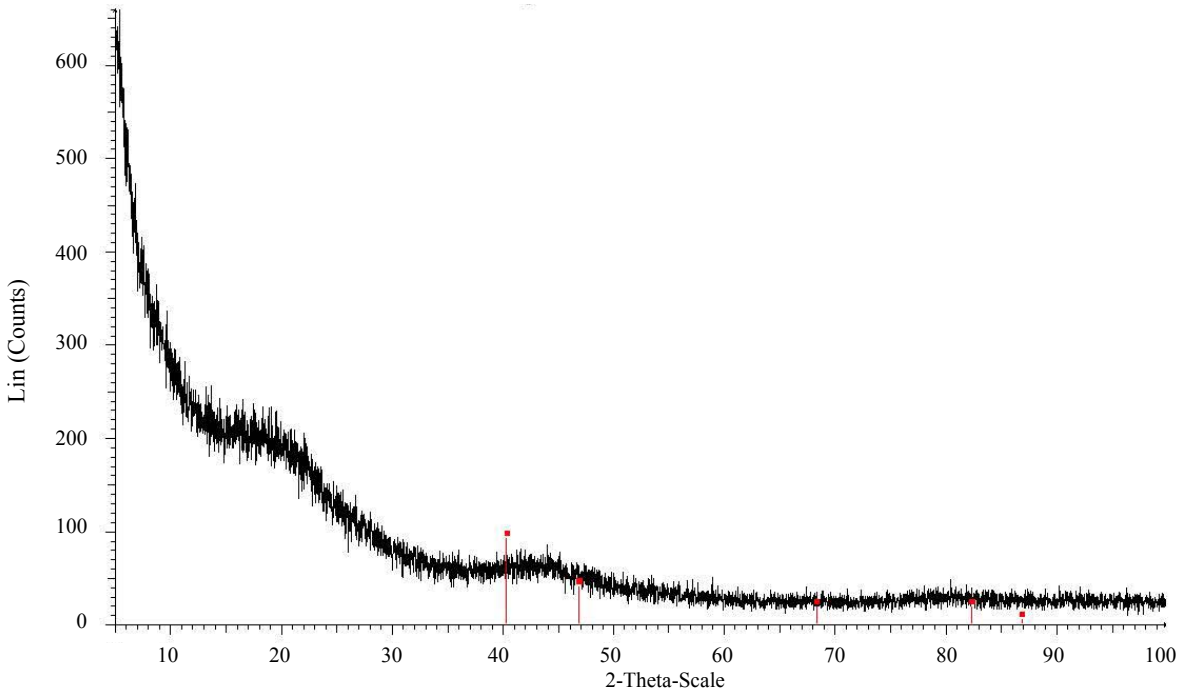

Figure 4.4 XRD data of bridged Maxsorb carbon

Figure 4.4 of bridged Maxsorb confirmed what had been observed with the bridged Black Pearls. There were no XRD peaks associated with Pd, which was again attributed to the very low wt.% of palladium deposited (0.44 wt.%), which was selected in order to match that used in the literature. It was not possible to calculate the Pd particle size from the full width half maximum due to the lack of peaks. However, it seems unlikely that the Pd grain/particle size would have changed from the starting material through the bridging process.

4.1.5 XRD of As-received and Bridged MOF-5

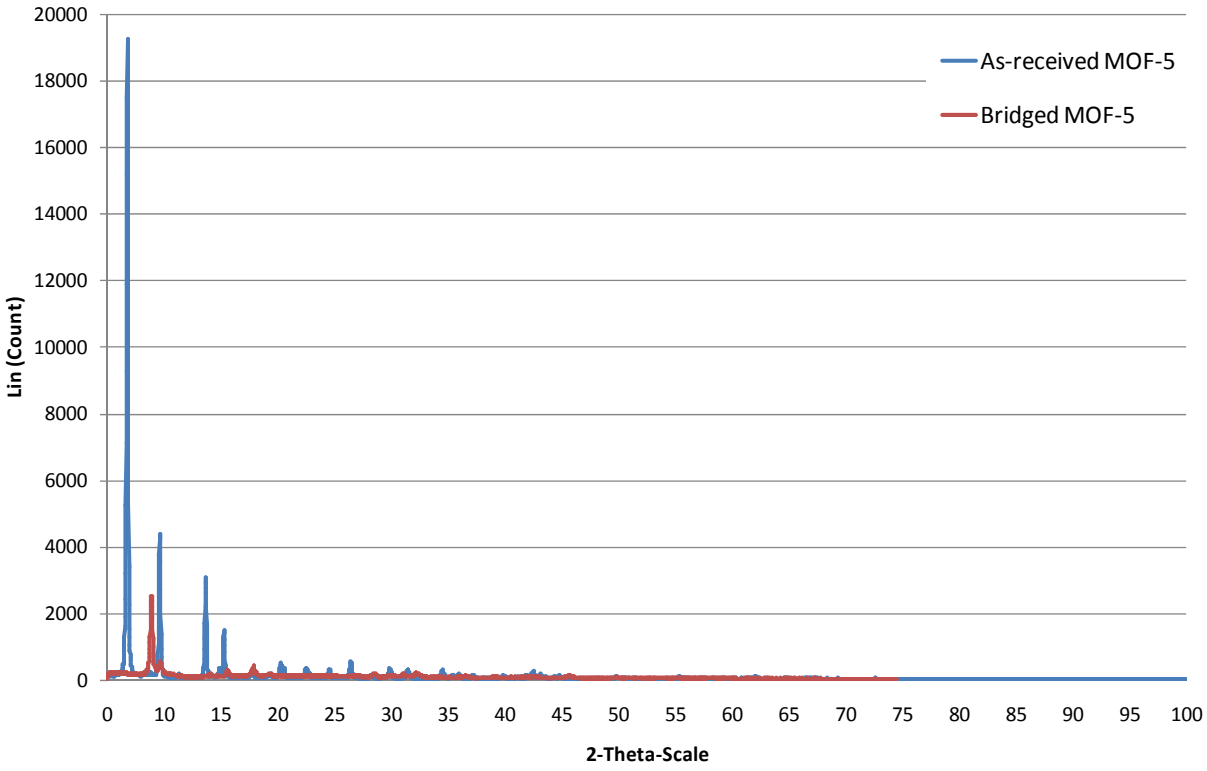

Figure 4.5 XRD data of as-received (blue) & bridged (red) MOF-5

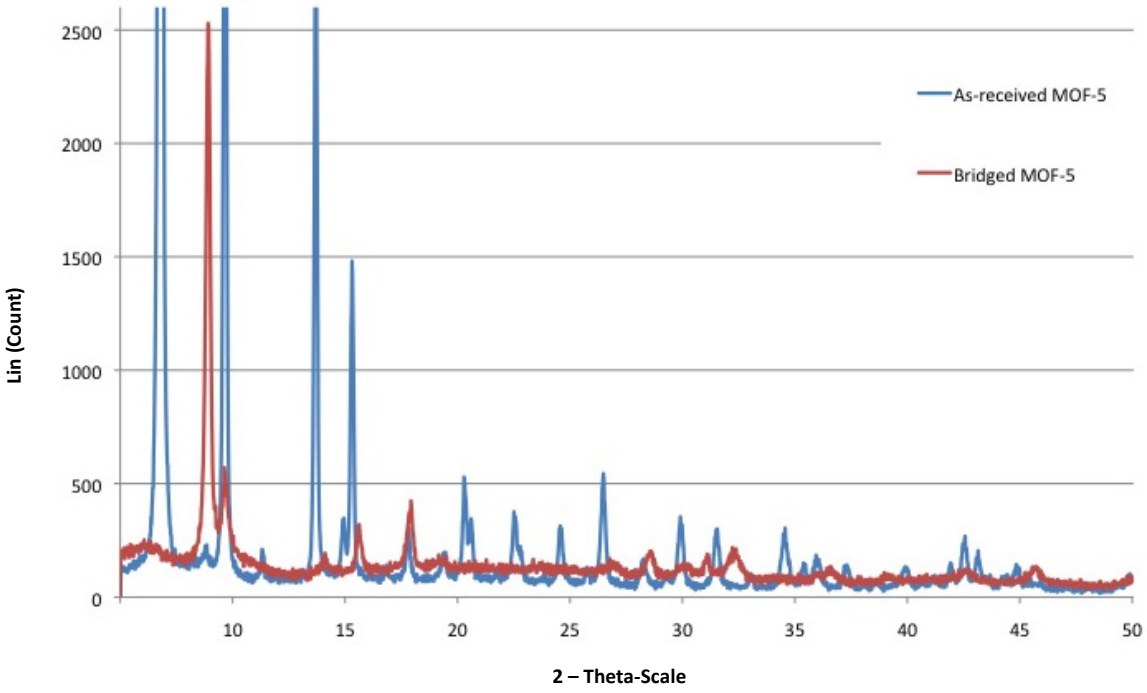

Figure 4.6 XRD data of magnified section of as-received & bridged MOF-5

Bridged MOF-5 (0.44 wt.%) also did not show any Pd XRD peaks, due to the low Pd wt.% content (see Figure 4.5). However, the XRD data did show a significant shift and reduction in intensity of the peaks (see Figure 4.6). This suggested that the bridging procedure, which included physical mixing/grinding in air with a mortar and pestle might well have damaged the highly ordered framework structure. This explanation was later confirmed by a corresponding reduction in surface area and consequent lower hydrogen uptake at 77 K (see section 4.2.4).

4.2 Hydrogen Storage Properties Of Materials

4.2.1 Hydrogen storage in As-received Palladium

Figure 4.7 shows the hydrogen uptake of as-received palladium powder (particle size <100μm) as measured on a Hiden HTP volumetric system up to 40 bar, to act as a baseline for high surface area materials.

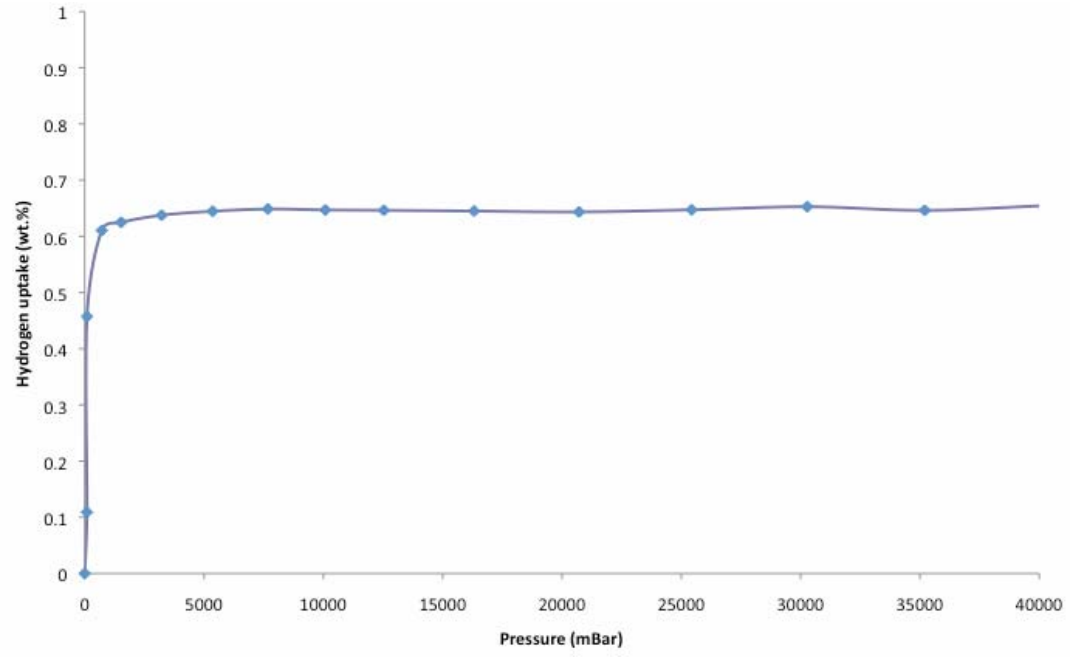

Figure 4.7 Absorption of H_2 in as-received palladium powder at 50°C, measured on a volumetric Hiden HTP system

The result showed the rapid uptake of hydrogen by palladium at very low pressures followed by a long plateau indicative of hydrogen saturation, which occurred effectively under 1 bar pressure of hydrogen and uptake was around 0.64 wt.% which is similar to the literature values of 0.66 wt.%[52]. The palladium particle size was found to be <100 μm, using a confocal laser microscope as shown in Figure 4.8 below.

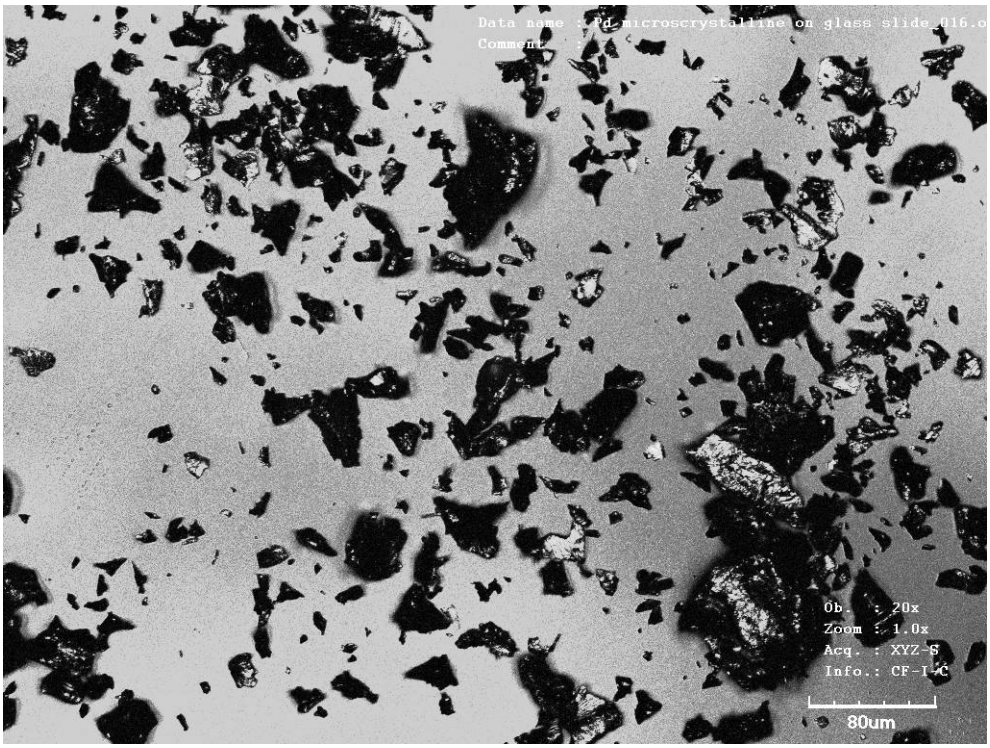

Figure 4.8 Image of palladium powder using a confocal microscope

Temperature Programmed Desorption (TPD) was also carried out to observe the hydrogen desorption behaviour over a range of temperatures. It showed two distinct hydrogen desorption peaks at around -100°C and 100°C. The two peaks of hydrogen desorption seen at -100ºC and 100ºC are very similar to those observed in the literature for bulk palladium hydride desorption[67].

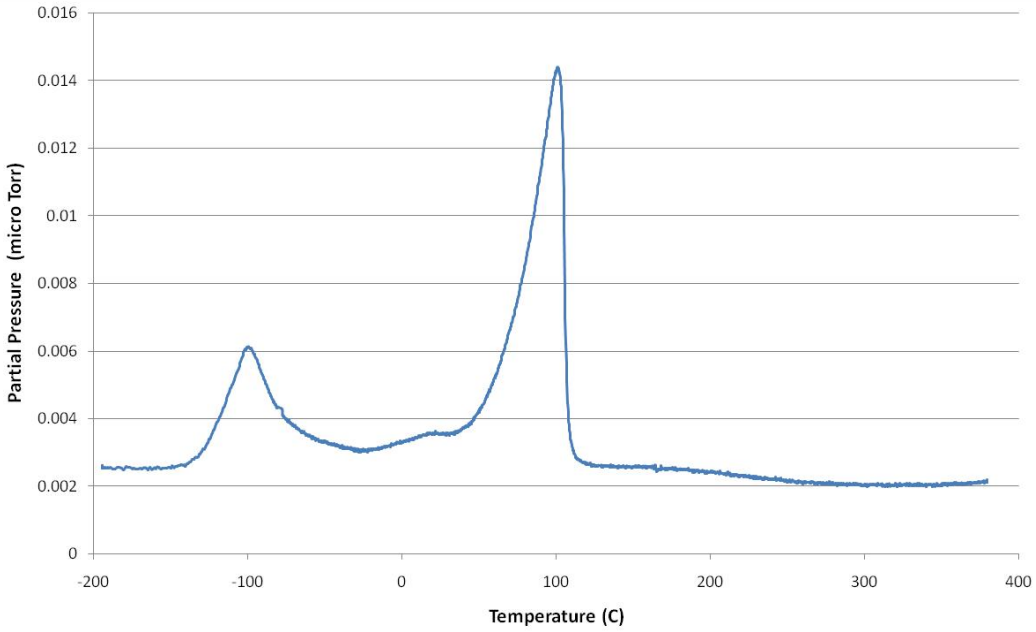

Figure 4.9 TPD of as-received palladium powder (hydrided for 6 hrs at 100 bar, then cooled to 79 K), heated at 5 K/min under He flowing at 5 cm^3/min

The first lower temperature peak in Figure 4.9 was attributed to the release of hydrogen from the near-surface hydride layer and the second was associated with the desorption of chemisorbed hydrogen[67]. The first peak is only visible when the palladium has been exposed to hydrogen below 140 K (-133 ºC)[67] which was the case in these conditions. The desorption characteristics seen are also a function of the palladium particle size and dispersion[55]. The peak intensities are dependent on the set-up parameters of the mass spectrometer, such as flow rate and vacuum levels. Since the palladium used to bridge the porous materials was of smaller particle size and in contact with a carbon support, it was expected that the desorption behaviour of these samples would be slightly different.

4.2.2 Hydrogen storage in Maxsorb

The skeletal density of as-received Maxsorb from the literature was 2.19 g/cm^3[3,16]. The hydrogen uptake of Maxsorb at room temperature was measured on both the IGA and HTP systems as shown in Figure 4.10 below.

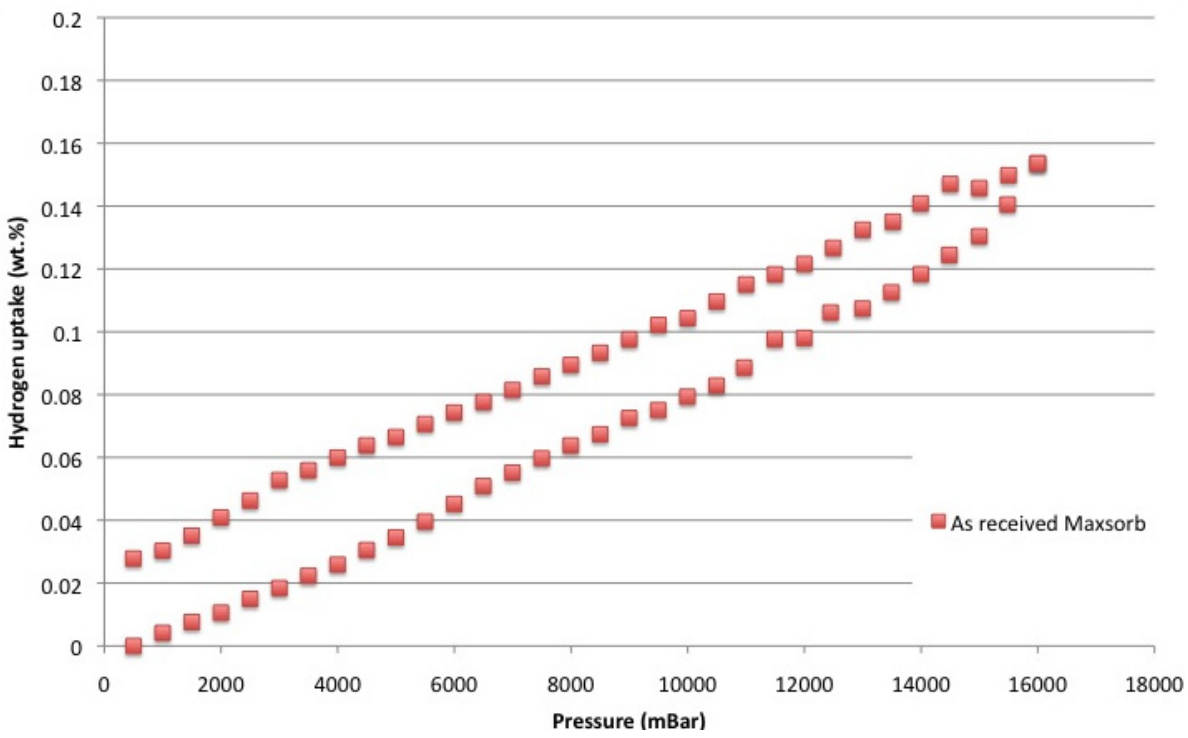

Figure 4.10 As-received Maxsorb hydrogen adsorption and desorption data run twice at room temperature (297 K) measured on a gravimetric Hiden IGA system

As expected for high surface area materials at room temperature, the uptake of hydrogen by as-received Maxsorb was low (0.15 wt.% at 16 bar), near linear and reversible. This is slightly higher than the reported value of 0.1 wt.% at 16 bar[17]. There was a little hysteresis on the as-received Maxsorb measurements, but this is relatively common for these types of high surface area materials with very small hydrogen uptakes at room temperature. More interestingly,

Maxsorb bridged with palladium showed only a slight improvement over the as-received sample (See Figure 4.11), which suggested that hydrogen spillover was not occurring using this bridging method.

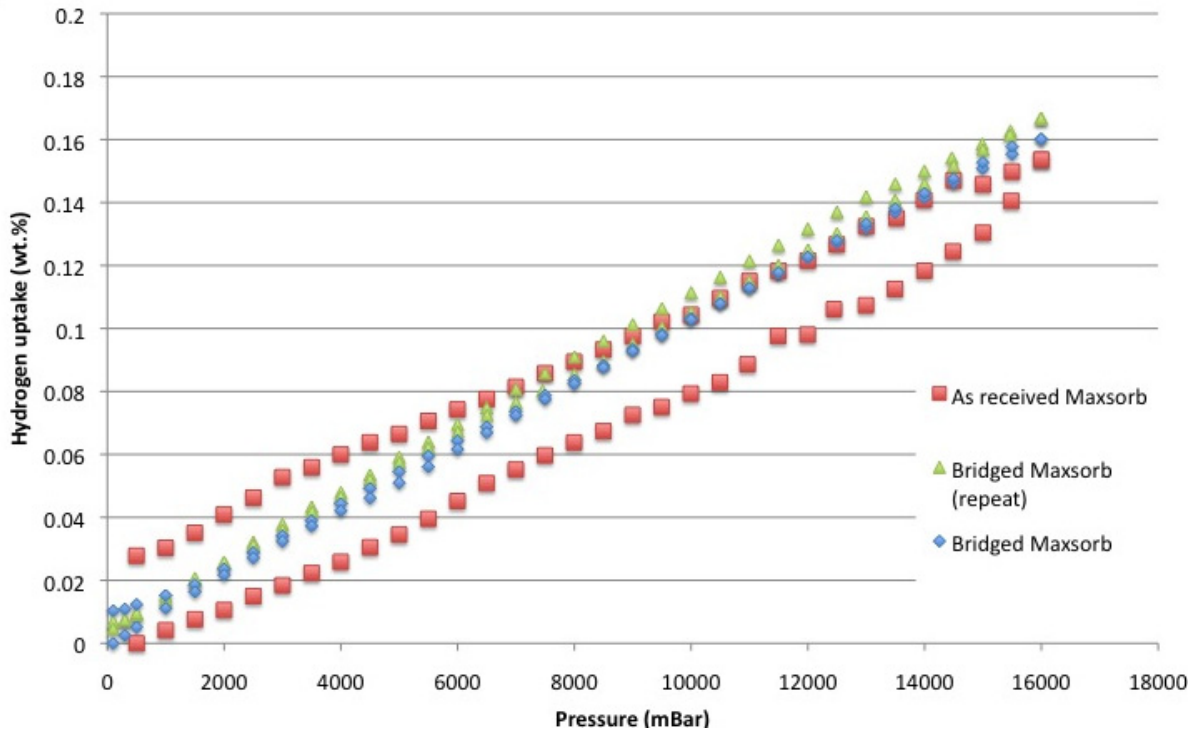

Figure 4.11 Bridged Maxsorb hydrogen adsorption and desorption at room temperature (295 K) measured on a gravimetric Hiden IGA system

The hydrogen uptake behaviour was also investigated at higher pressures on the HTP system (see Figure 4.12 below) to observe any changes in the adsorption profile and to examine how accurately the IGA (gravimetic) and HTP (volumetric) systems compared.

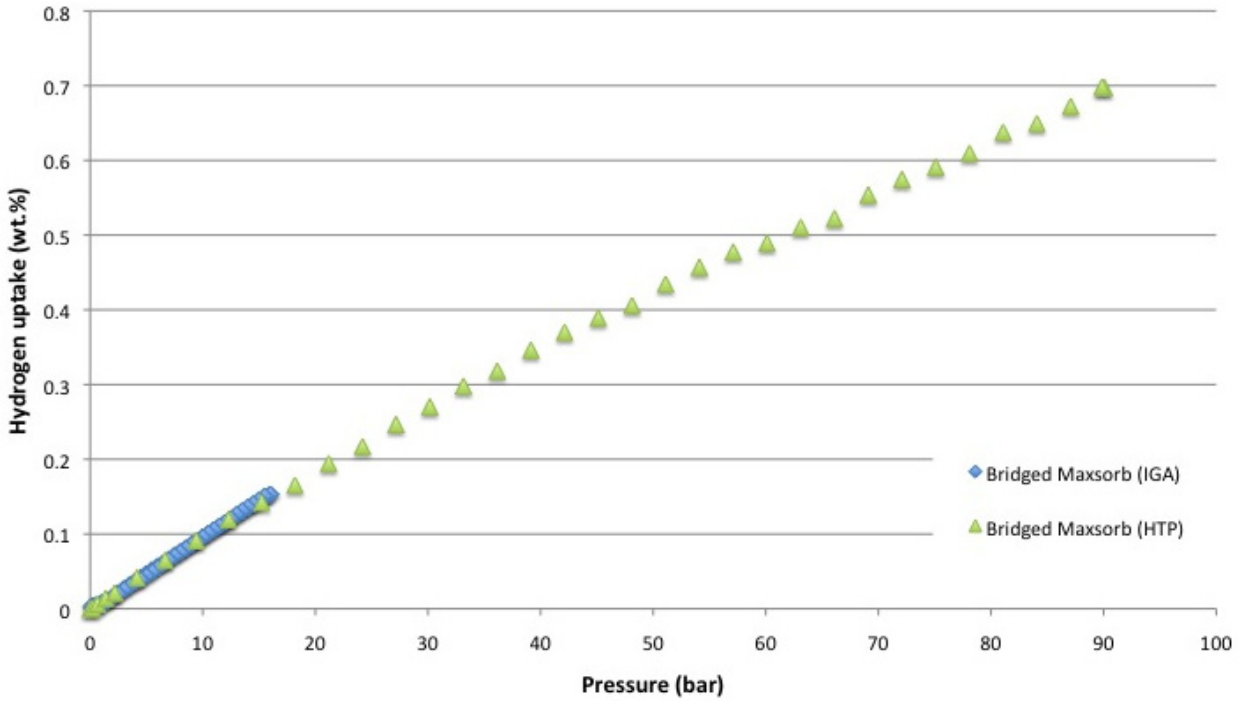

Figure 4.12 Hydrogen adsorption of Bridged Maxsorb at room temperature (302 K), measured on a gravimetric Hiden IGA (up to 16 bar) and on a volumetric Hiden HTP system (up to 90 bar)

The results firstly show that the relationship between uptake and higher pressures was nearly linear at these pressures, which means the saturation pressure was not reached and must therefore be extremely high, which has also been observed in the literature[17]. Secondly, it was shown that up to 16 bar the hydrogen uptake was very similar when compared on the HTP and IGA systems. As-received Maxsorb must also be measured at higher pressures to compare the effects of bridging with palladium at these higher pressures. Given that the results of the IGA and HTP were reasonably consistent up to 16 bar for this sample, the IGA was used when possible to avoid methodological problems associated with the HTP system (see appendix).

4.2.3 Hydrogen storage in Black Pearls 2000

The hydrogen storage properties of as-received Black Pearls 2000 were also investigated using the IGA system to serve as a standard for the bridged and chemically doped samples.

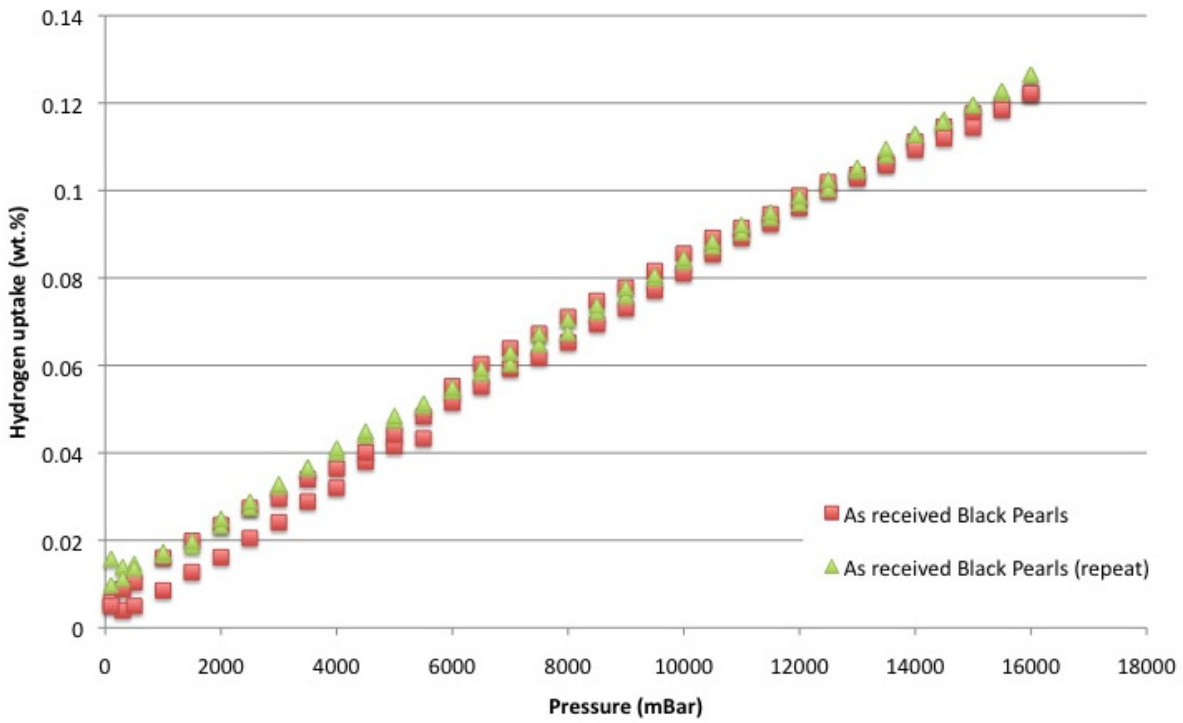

Figure 4.13 Hydrogen adsorption and desorption on as-received Black Pearls run twice at room temperature (296 K), measured on a gravimetric Hiden IGA system

Similarly in Figure 4.13, the hydrogen uptake at room temperature was very low, near linear and reversible. The uptake at 16 bar for as-received Black Pearls was 0.12 wt.%. This was slightly lower than the as-received Maxsorb sample which adsorbed 0.16 wt.% at 16 bar. This difference was attributed to the lower surface area, which provided fewer sites for surface physisorption. The as-received Black Pearls was then compared to bridged Black Pearls as shown below in Figure 4.14.

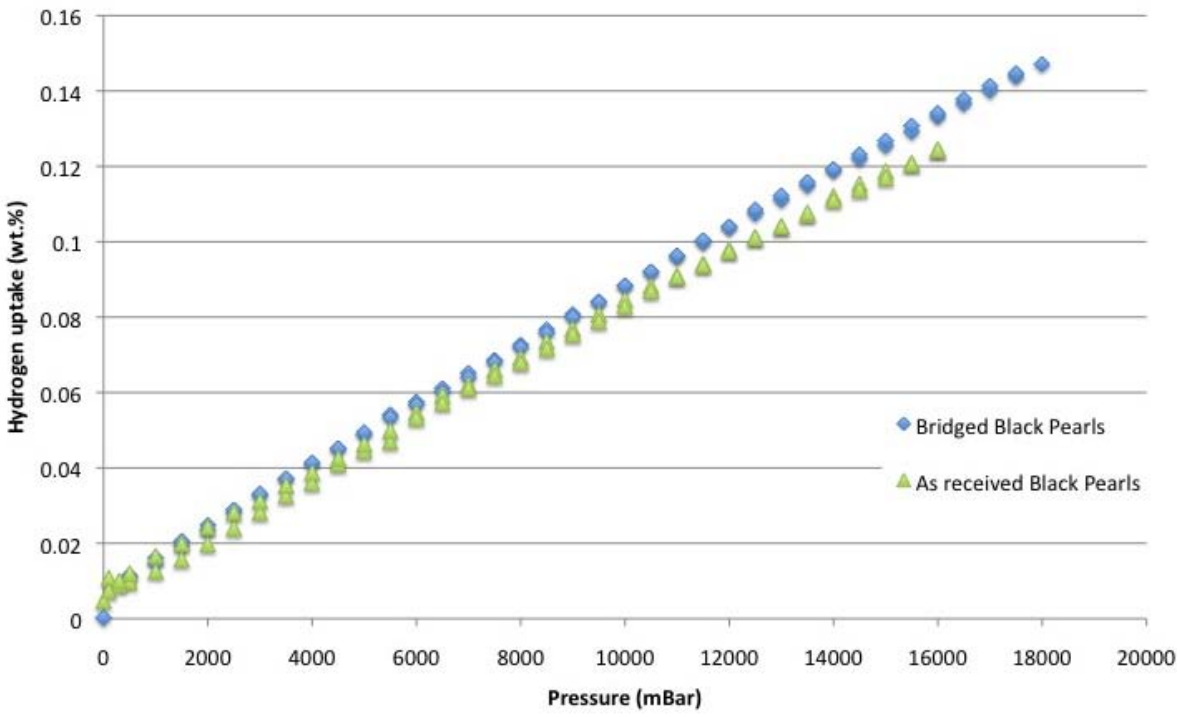

Figure 4.14 Hydrogen adsorption and desorption on as-received and Pd-bridged Black Pearls at room temperature (291 K), measured on a gravimetric Hiden IGA system

The results show that the as-received and Pd-bridged Black Pearls carbon samples have very similar hydrogen uptake behaviour. There did not seem to be a significant hydrogen adsorption enhancement (under these conditions), after bridging with small amounts of palladium. This was not consistent with the literature[40] that showed an enhancement by a factor of 2.9 for another high surface area carbon (AX-21) at 298 K and 60 bar with the same level of Pd-doping.

The reason for the lack of significant enhancement on both carbons may well have been that the bridges between the 5 wt.% Pd/C and carbon receptors were not formed. This is suggested because these marginally higher results for hydrogen uptake bear a closer resemblance to physically mixed Pd and carbon[40] rather than bridged. Alternatively, it is possible that the

palladium may have been in some measure encapsulated by carbon during the bridging process causing a reduction hydrogen uptake[56]. However, both of these possibilities should be tested by the use of direct observation, such as SEM.

An alternative approach to investigate hydrogen spillover was by chemically doping Black Pearls carbon with Pd, using a proprietary technique at Johnson Matthey, resulting in a chemically-doped sample that consisted of 6 wt.% Pd. The density of this Johnson Matthey chemically doped Black Pearls sample was calculated to be 2.47 g/cm^3 using He pycnometry. The uptake results were compared to the previous as-received and Pd-bridged samples in Figure 4.15 below.

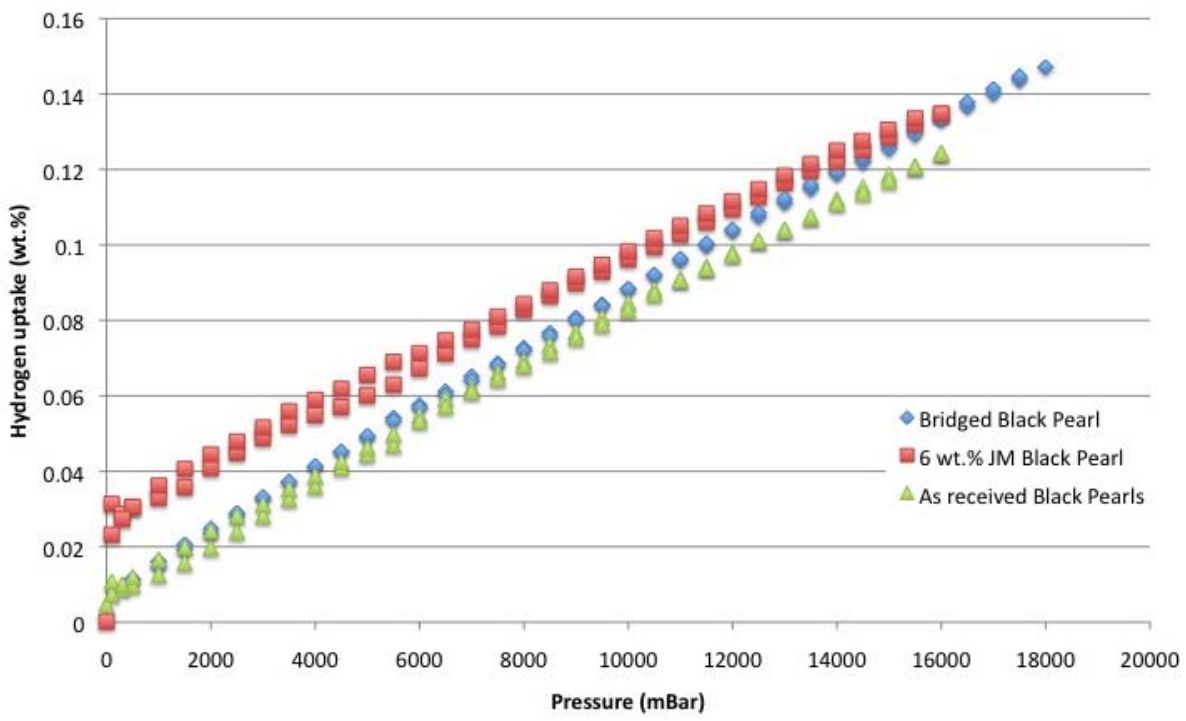

Figure 4.15 Hydrogen adsorption and desorption of different types of Pd-doped Black Pearls carbon at room temperature, measured on a gravimetric Hiden IGA system

The Johnson Matthey 6 wt.% Pd Black Pearls showed an initial rapid uptake rate at very low pressures (<1 bar) followed by a return to similar adsorption rates observed for the as-received and bridged samples. This uptake behaviour seems to be consistent with an initial hydrogen absorption by palladium at low pressures followed by linear adsorption on carbon. This suggests that the palladium and carbon support are sorbing hydrogen independently, rather than hydrogen spilling over from the palladium to the carbon support. The hydrogen uptake of the palladium exclusively in this sample can be estimated because it is 6 wt.% of the total mass of 122 mg, which corresponds to 7.32 mg of palladium. If the palladium absorbs approximately 0.6 wt.% of hydrogen (see section 4.2.1), then it would be expected to absorb around 0.0439 wt.% of hydrogen. This estimate of hydrogen uptake exclusively by palladium shows some resemblance to the initial uptake of the 6 wt.% Pd Black Pearls sample. A similar double uptake response has been observed by Lachawiec et al.[40] and Anson et al. [17] at low pressures (<1 bar) on carbons doped with higher loadings of Pd. However the initial hydrogen uptake of a 5 wt.% Pd on activated carbon (Lachawiec et al.[40]) and the overall hydrogen uptake at higher pressures were both significantly higher than that observed in this work. Temperature Programmed Desorption measurements were then carried out (see Section 3.2.3) to observe the desorption characteristics of this sample and the response was compared to that of the as-received Pd powder in Figure 4.16 below.

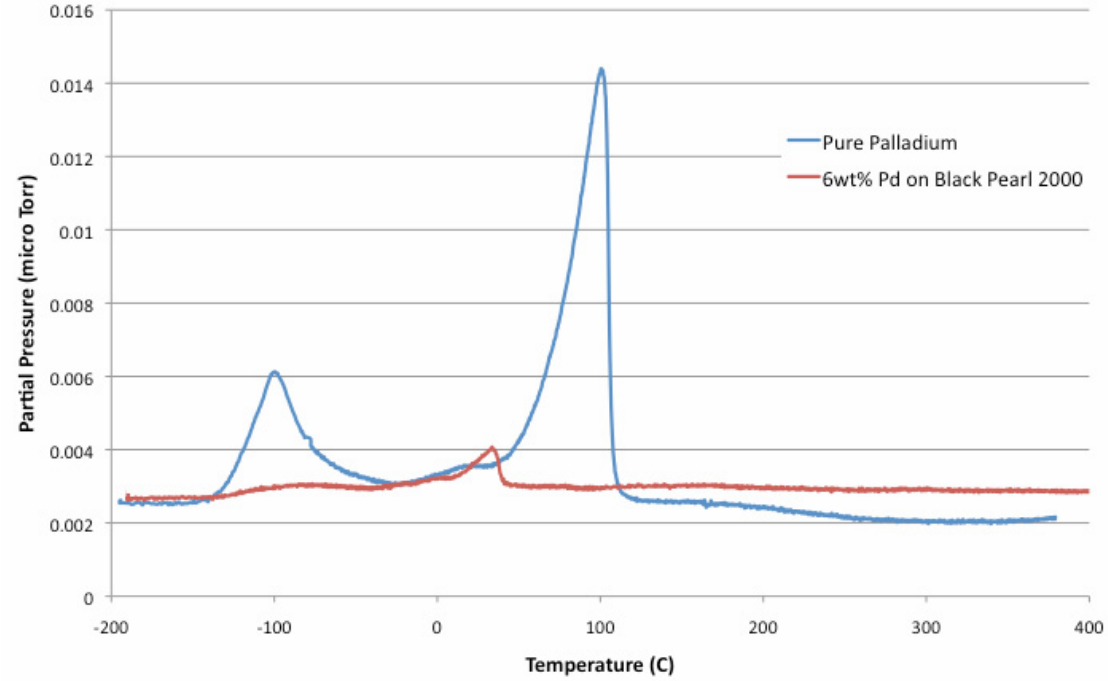

Figure 4.16 TPD of as-received Pd and Johnson Matthey Black Pearls carbon chemically doped with Pd

Figure 4.16 shows an obvious peak at around 30 °C for the desorption of hydrogen from the sample which was lower than previously seen from (100 °C) with the as-received palladium. Amorim & Keane[52] have also found that the temperature for maximum hydrogen release/hydride decomposition was lower for supported palladium than bulk palladium. This suggests that the presence of a support is having an effect on the desorption of hydrogen from the palladium. The first very low temperature peak for as-received palladium was difficult to distinguish, suggesting that the contact with the carbon support had inhibited the hydrogen being released from the near surface hydride layer. The difference in intensity of the peaks between the two samples was attributed to the smaller amount of palladium used in the chemically doped sample compared to the as-received palladium powder.

4.2.4 Hydrogen storage in MOF-5

The density of as-received MOF-5 and bridged MOF-5 were calculated using a He pycnometer to be 1.98 g/cm^3 and 1.99 g/cm^3 respectively. Hydrogen uptake measurements on as-received and bridged MOF-5 were carried out using a Hiden IGA system up to 18 bar (see Figure 4.17).

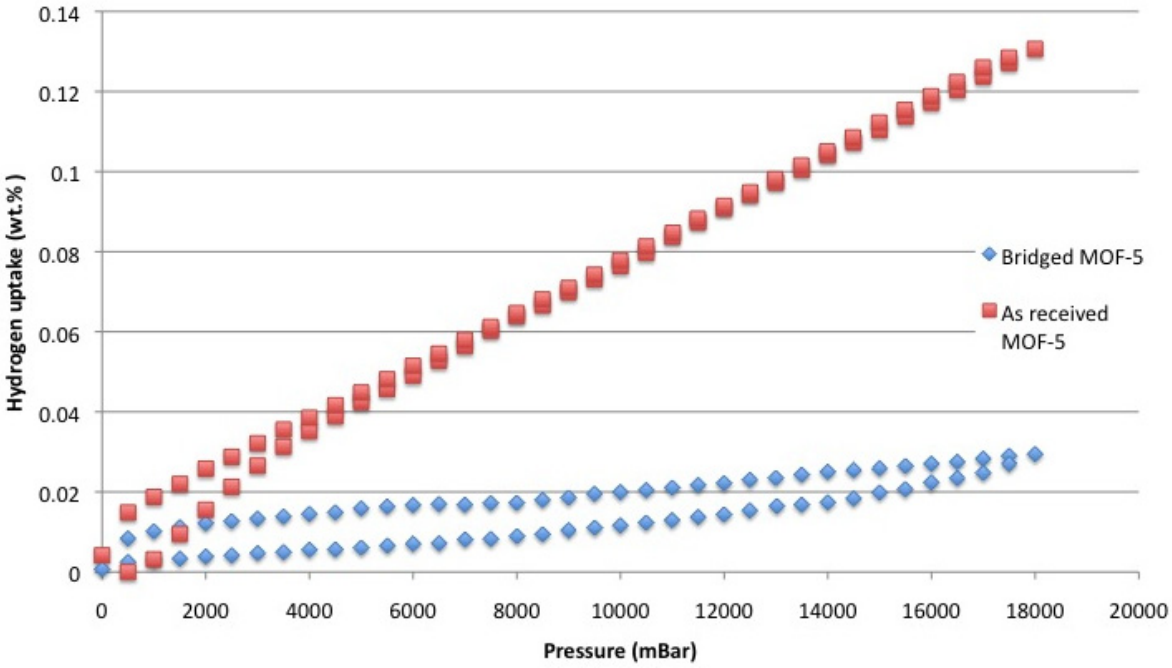

Figure 4.17 Hydrogen adsorption and desorption of as-received and Pd-bridged MOF-5 at room temperatures (295 & 296 K) measured on a Hiden IGA system

The uptake of hydrogen at room temperature for as-received MOF-5 was again low (0.13 wt.% at 18 bar), near linear and reversible. However, the uptake of bridged MOF-5 at 0.03 wt.% was significantly lower. Therefore, it seemed likely that the bridging process had damaged the complex structure of the metal organic framework, resulting in the reduction of surface area and consequently in hydrogen uptake. To confirm if this was actually the case, hydrogen isotherms were measured at 77 K on both as-received and bridged MOF-5 up to 18 bar (see Figure 4.18). As-received MOF-5 has been well characterized at these temperatures

and pressures, typically adsorbing 5 wt.% at 77 K and 50 bar[68]. Hydrogen uptake at 77 K for high surface area MOF materials can be roughly correlated to surface area, 1.5 wt.% uptake corresponding to 1000 m^2/g of surface area[69,8].

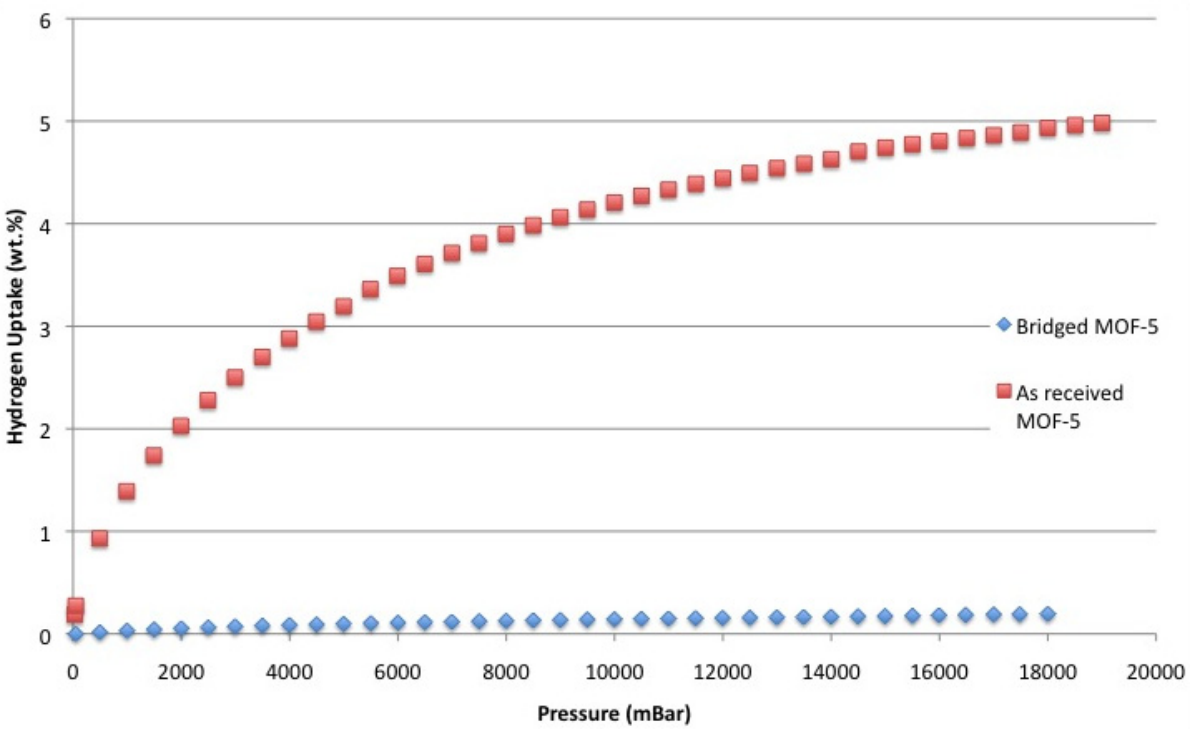

Figure 4.18 Hydrogen adsorption of as-received and Pd-bridged MOF-5 at 79 K measured on a gravimetric Hiden IGA system

The isotherms showed that bridged MOF-5 only adsorbed ~0.2 wt.% at 77 K in contrast to 5 wt.% for as-received MOF-5. This suggests that the surface area of the bridged MOF-5 has been drastically reduced by the bridging procedure as there are far fewer sites for physisorption and consequently hydrogen storage was lower. Using the approximate relationship between surface area and hydrogen uptake at 77 K, the bridged MOF-5 with a hydrogen uptake of 0.2 wt.% could be expected to have a surface area of ~120 m^2/g. This significant surface area change following the bridging procedure, agrees with the XRD data in section 4.1.5 that showed significant structural change had occurred. These results of significantly reduced surface area contradict the literature on Pt doped MOFs,[42] on which the

mixing procedure (physical mixing with mortar and pestle in air) was based. This method is difficult to reproduce exactly due to the unquantifiable nature of physical mixing with mortar and pestle. A very recent paper by Miller et al.[70] who used ball milling in a helium atmosphere on IRMOF-8 suggests that the damage done to the framework was caused by the exposure to air rather than physical mixing.

4.2.5 Summary of hydrogen storage in Pd bridged materials

Figure 4.19 summarises the hydrogen storage measurements of as-received and Pd-bridged samples at 16 bar (1.6 MPa) at 298 K.

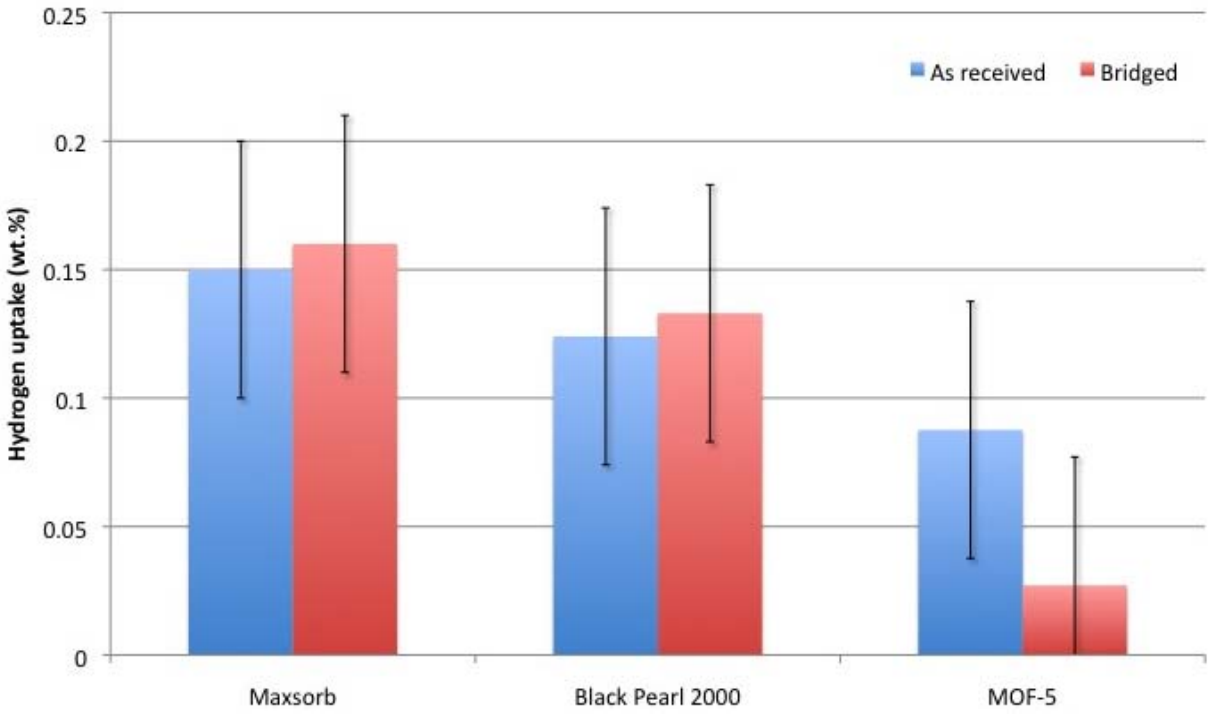

Figure 4.19 Average hydrogen uptake values for as-received, Pd-bridged (0.44 wt.%) samples at room temperature and 16 bar

Figure 4.19 shows that there was only a marginal improvement in room temperature hydrogen uptake for the two carbon samples bridged with very small amounts of palladium over the as-

received samples. The ± 0.05 wt. % error bars were used from previous research on hydrogen storage using the same IGA system[71]. The marginal improvement observed for palladium bridged carbons is contrary to much literature earlier reviewed (Section 2.6) which saw much larger enhancements that were attributed to hydrogen spillover. This seems to suggest that the formation of bridges between palladium and carbon were not formed in this work and consequently highlights that the bridging procedure is critical for the spillover of hydrogen. The Johnson Matthey chemically doped carbon also showed no significant enhancement in overall hydrogen storage. It is difficult to speculate why this was the case as the exact synthesis conditions were unknown. Additionally, the quality of contact between the palladium particles and carbon was unknown which could have inhibited the hydrogen spillover mechanism if the contact was poor. In contrast to the bridged and chemically doped carbon results, Pd-bridged MOF-5 showed a significant reduction in hydrogen storage capacity. This was attributed to a structural change brought about by the mixing procedure as observed by changes in XRD peak data between as received and bridged MOF-5.

5 - CONCLUSION

This research primarily aimed to investigate the presence and significance of hydrogen spillover in palladium doped high surface area materials through bridged and chemical doping.

XRD was unable to be used to identify palladium dopants on the receptor materials after bridging Pd/C onto Maxsorb (activated carbon), Black Pearls 2000 (carbon furnace black) and MOF-5 samples. This was attributed to the very small wt.% of palladium used. However, palladium peaks were observed on the Johnson Matthey chemically doped Black Pearls sample of higher palladium content (6 wt.%). Unfortunately, the XRD data for MOF-5 showed signs of significant structural change following the bridging process that involved physical grinding in air.

Hydrogen adsorption measurements were carried using gravimetric (Hiden IGA) and/or volumetric (Hiden HTP) systems at room temperature for the carbon and MOF samples. As expected as-received Maxsorb, Black Pearls and MOF-5 uptakes were all very low at room temperature (0.1 - 0.2 wt.%). A comparison of the hydrogen uptake of an identical Maxsorb sample on both the gravimetric (IGA) and volumetric (HTP) systems suggested that comparable results were obtainable from the two different techniques (upto the maximum operating pressure of the IGA of 20 bar). Experimental errors including corrections, impurities and leaks were potentially significant especially when measuring very low hydrogen uptakes. However, a number of precautions were taken to minimise them, including the use of high purity gases, liquid nitrogen traps and appropriate fittings.

Bridging the Black Pearls and Maxsorb carbon samples with 5 wt.% Pd/C, using the method in the literature[40], resulted in a fractionally higher hydrogen uptake at 16 bar which was near linear in nature. This was different to the literature[40] which saw a slightly steeper initial uptake at very low pressures (0.25 bar) and a sustained further enhancement up to 100 bar. The reason for the lack of significant enhancement may well have been that the bridges between the 5 wt.% Pd/C and carbon receptor were not formed, which is supported by this work bearing a closer resemblance to physically mixed 5 wt.% Pd and carbon[40]. Alternatively the palladium may have been in some measure encapsulated by carbon during the bridging process causing a reduction hydrogen uptake.

The bridging process for MOF-5 resulted in a significant decrease in hydrogen uptake when compared with as-received MOF-5. This was attributed to a reduction in surface area brought about by damage due to the mixing process used in previous literature[41], as shown by a greatly reduced hydrogen uptake at 77 K. The reason why an enhancement was not seen despite the replication of the method was suggested to be the detrimental process of physical mixing in air.

When the higher 6 wt.% Pd chemically doped Black Pearls sample was measured, an initial rapid hydrogen uptake was observed (<1 bar) followed by a shallower near linear uptake. A similar double uptake response has been observed by Lachawiec et al.[40] and Anson et al. [17] at low pressures (<1 bar) on carbons doped with higher loadings of Pd. However the initial hydrogen uptake and the overall uptake at higher pressures found for a 5 wt.% Pd on activated carbon (Lachawiec et al.[40]) were both significantly higher than that observed in this work. The hydrogen uptake from the 6 wt.% chemically doped Black Pearls sample seems more

consistent with palladium and carbon independently sorbing hydrogen, rather than hydrogen spilling over from the palladium to the carbon support giving improved uptake. However, this tenuous result must be further replicated to establish the validity of this conclusion. In addition the synthesis conditions must be clarified and the material examined by SEM to ensure that there is indeed a good Pd/carbon interface.

Temperature Programmed Desorption (TPD) measurements compared the desorption of hydrogen from Pd powder and 6 wt.% Pd Black Pearls. The presence of a carbon support resulted in a reduction of the low temperature peak associated with near surface hydrogen and a lowering of the temperature for maximum hydrogen desorption from 100 °C to 30 °C suggesting an important interaction between palladium and carbon. The parameters of this interaction need to be further examined. Amorim & Keane[52] have suggested that any hydrogen desorbed from the carbon support would occur above the maximum operating temperature of 773 K for the Hiden system.

6 - FUTURE WORK

There is much future work that is needed to further clarify the nature of the hydrogen spillover mechanism in the porous hydrogen storage materials examined. This may include the investigation of:

- The repetition of Johnson Matthey chemically doped Black Pearls 2000 to verify the conclusion that spillover was not occurring under these conditions. This would also involve clarification of synthesis conditions and SEM to ensure that the palladium particles are actually in good contact with carbon support.
- Very low-pressure (0-1 bar) measurements with low pressure transducers for greater accuracy on all samples to observe more clearly the effect of palladium.
- High-pressure HTP measurements on as-received Maxsorb and Black Pearls samples to check hydrogen sorption behaviour at higher pressures.
- Higher wt.% of palladium (e.g. 5 wt.%) to bridge the receptor materials in order to see more clearly the effects of doping.
- The use of other catalysts for spillover such as platinum, which does not form hydrides and may have different hydrogen dissociation mechanisms to palladium.
- Modification of the doping technique for MOF-5, specifically, mixing in an inert atmosphere to avoid the degradation of the framework structure.
- A more reproducible method for physical mixing of carbon receptors used such as mechanical mixing.
- Synthesis conditions needed to achieve bridging and analysis of the resulting "bridges" by FTIR or Raman.

- The effects of repeatedly adsorbing and desorbing to examine if there are any cycling effects.
- Measuring the surface areas of samples to see how much of a detrimental impact doping with Pd had on surface area.
- TEM to further characterize material properties including particle size, dispersion and the nature of deposition in receptor materials.
- The Pd/carbon interaction and the effect of Pd particle size on hydrogen absorption and desorption with Temperature Programmed Desorption (TPD).
- Calculation of the heats of desorption of various doped receptors to find near ambient temperature desorption behaviour.
- TPD of hydrogen to higher temperatures to show the desorption of hydrogen from both the palladium and the support.
- The pyrolysis conditions of the carbonized bacteria in order to increase the surface area and consequently the hydrogen storage capacity.

7 - APPENDIX

7.1 Chemical doping method for MOF-5

A chemical method was also attempted for doping a MOF-5 sample at Johnson Matthey. An amine group was used in order to promote the attachment of palladium nanoparticles to the MOF-5 structure. MOF-5 was prepared by two solutions of 0.498 g of $Zn(NO_3)_2.6H_2O$ in 10 ml of DEF (diethylformamide) and 0.666 g of the ligand in 50 ml of DEF. The ligand was heated to 373 K and then the zinc solution was added. The solution was then left for 5 hrs. After this time the solution was filtered by vacuum filtration and washed with chloroform. Pd nanoparticles were prepared by using 0.1 g of $Pd(acac)_2$ in 20 ml of a confidential amine. The temperature was then increased to 403 K for 30 minutes, centrifuged to remove the amine, suspended in 30 mls of toluene and sonicated for 10 minutes. The nanoparticles solution was then added to the MOF-5 powder and stirred overnight. The resulting solution was then vacuum filtered. Unfortunately, this process did not yield sufficient quantities for the characterisation of the resulting materials hydrogen sorption properties.

7.2 Methodological problems associated with the HTP system

The large pressure changes associated with the HTP volumetric technique resulted in the propulsion of some of the sample out of the sample container through 0.5 μm filter and into the machines pipework. This was also found to be the case even when using ceramic wool and anti bumping alumina beads to trap the sample. A secondary 0.5 μm microfilter was fitted to reduce the likelihood of damage to the HTP system. However this resulted in a diminished flow rate which was a particular problem for the TPD which required a higher flow rate.

7.3 Hydrogen storage in Pd-doped carbon made from pyrolysed bacteria

The hydrogen storage properties of Pd-doped carbon made from pyrolysed bacteria were measured using a Hiden IGA. However, the BET surface area was calculated to be only about 1.5 m^2/g, which is much too low to be useful as a substrate support for hydrogen storage materials. A hydrogen adsorption isotherm showed that the overall adsorption was negligible (highest of ~0.018 wt.%) at 298 K and 1 bar as shown in Figure 7.1 below.

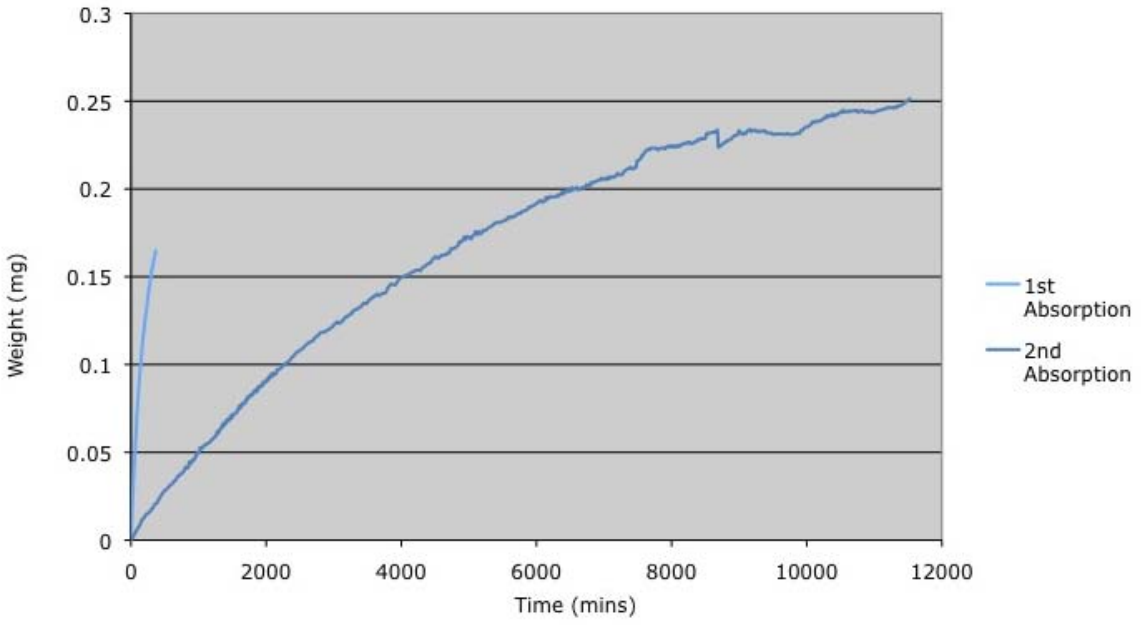

Figure 7.1 Hydrogen adsorption isotherm for Pd doped carbon made from pyrolysed bacteria at 298 K and 1 bar measured on the Hiden IGA system

The most probable explanations for the very low uptake of hydrogen are the very low surface area of the pyrolysed bacteria and the low pressures used. It is also possible that the palladium was enveloped in carbon through the biosynthetic process as it has been shown[61] that palladium nanoparticles are formed in the outer layers of the cell wall (see Figure 7.2). A reference material of carbon made from pyrolysed bacteria without palladium was not used and so conclusions are limited.

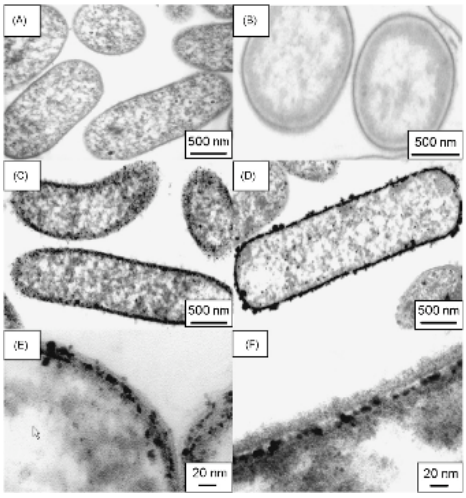

Figure 7.2 TEM of Pd nanoparticles in the cell walls of bacteria[72]

The Temperature Programmed Desorption (TPD) trace of bio palladium showed a leftward shift of the two desorption peaks. The difference in intensity of peaks was attributed to the different flow rates to the mass spectrometer rather than the quantity of palladium. Interestingly, the maximum peak for desorption was the low temperature peak (-140 °C) which has been associated with near surface hydrogen which shows that the carbon made from pyrolysed bacteria is influencing the desorption behaviour of palladium. A TPD of carbon made from pyrolysed bacteria should also be carried out for further comparison.

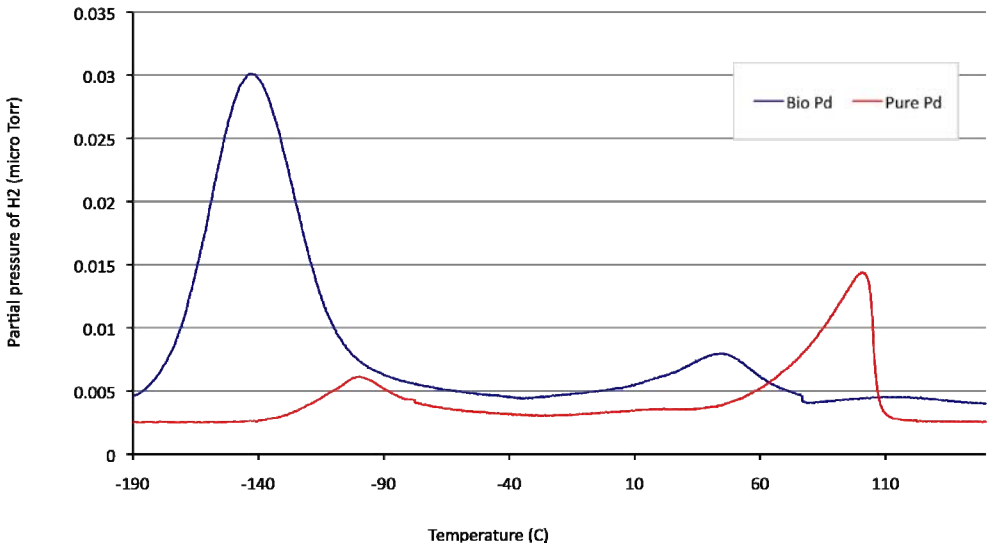

TPD of as-received and Pd powder and Pd-doped carbon made from pyrolsyed bacteria, from -190 to 120 °C measured on the Hiden HTP

REFERENCES

[1] Intergovernmental Panel on Climate Change (2007), *Climate Change 2007* Fourth Assessment Report, http://www.ipcc.ch/ipccreports/assessments-reports.htm, *accessed August 2008*

[2] D. Lüthi, M. Le Floch, B. Bereiter, T. Blunier, J. M. Barnola, U. Siegenthaler, D. Raynaud, J. Jouzel, H. Fischer, K. Kawamura & T. F. Stocker (2008) *Nature* **453**, p. 379-382

[3] Health Effects of Climate Change in the UK (2008), UK Department of Health

[4] International Energy Outlook (2008) US Energy Information Adminstration, http://www.eia.doe.gov/oiaf/ieo/highlights.html, *accessed August 2008*

[5] http://www.bp.com/genericarticle.do?categoryId=98&contentId=7033952, *accessed August 2008*

[6] N.H. Stern (2007) T*he Economics of Climate Change: The Stern Review,* Cambridge University Press

[7] P.M. Mathias & L.C. Brown (23 March 2003) "Thermodynamics of the Sulfur-Iodine Cycle for Thermochemical Hydrogen Production", presented at the 68th Annual Meeting of the Society of Chemical Engineers, Japan

[8] K.M. Thomas (2007) *Catalysis Today*, **120**, p.389-398

[9] A.C. Dillon K.M. Jones, T.A. Bekkedahi, C.H. Kiang, D.S. Bethune, M.J. Heben (1997) *Nature*, **386**, p.377-379

[10] A. Chambers, C. Park, R. T. K. Baker and N. M. Rodriguez (1998) *Journal of Physical Chemistry B,* **102**, p.4253-4256

[11] K.M. Thomas (2009) *The Royal Society of Chemistry, Dalton Transactions* p.1487–1505

[12] Z. Yang, Y. Xia & R. Mokaya (2007) *Journal of the American Chemical Society*, **129**, p.1673-1679

[13] N. Krishnankutty & M.A. Vannice (1995) *Journal of Catalysis*, **155**, p.312-326

[14] H.W. Langmi (2004) PhD Thesis, The University of Birmingham

[15] T. Otowa, R. Tanibata & M. ltoh (1993) *Gas Separation & Purification,* **7**, p.241-245

[16] Y. Takeuchi, M. Hino, Y. Yoshimura, T. Otowa, H. Izuhara & T. Nojima (1999) *Separation and Purification Technology,* **15**, p.79-90

[17] A. Anson, E. Lafuente, E. Urriolabeitia, R. Navarro, A.M. Benito, W.K. Maser and M.T. Martinez (2006) *Journal of Physical Chemistry B,* **110***,* p.6643-6648

[18]http://www.cea.fr/content/download/3112/14773/file /061a063pehr.pdf, *accessed September 2008*

[19] M. Hirscher & B. Panella (2007) *Scripta Materialia,* **56,** p.809–812

[20] A.G. Wong-Foy, A.J. Matzger, & O.M. Yaghi (2006) *Journal of the American Chemical Society,* **128**, p.3495

[21] A. Walton, S. Tedds & D. Book, (2009) *To be published in the Journal of Alloys & Compounds*

[22] S. Satyapal (2007) *DOE Hydrogen Program Merit Review and Peer Evaluation Meeting*

[23]http://nsm.raunvis.hi.is/~nsm/abstracts/M3-HydrNanoPorpous%2072/Poster/CZloteaNESSHYtest.pdf, *accessed January 2009*

[24] DOE Annual Merit Review in Washington, D.C., NREL presentation, May 16-19th, 2006

[25] Conner, W.C (Ed.) (1984) *Proceedings from the 1st International Conference on Spillover, Lyons, France,* University of Claude Bernard, Lyon-Villeurbanne

[26] A. Borgschulte, R.J. Westerwaal, J.H. Rector, H. Schreuders, B. Dam & R. Griessen (2006) *Journal of Catalysis***, 239**, p.263-271

[27] A.D. Leuking & R.T. Yang (2004) *Applied Catalysis A: General,* **265**, p.259-268,
[28] G.M. Pajonk (2000) *Applied Catalysis A: General,* **202,** p.157-169
[29] P.H. Emmett (1940) *Twelfth Report of the Committee on Catalysis (National Research Council);* John Wiley & Sons: New York p.64
[30] S. Koobiar (1964) *Journal of Physical Chemistry,* **68**, p.411- 412
[31] A.J. Robell, E.V. Ballou, & M. Boudart (1964) *Journal of Physical Chemistry,* **68**, p.2748
[32] M. Boudart, M.A. Vannice & J.E. Benson, (1969) *Z. Phyls. Chem. N.F.* **64**, p.171
[33] M. Boudart, A.W. Aldag & M.A. Vannice, (1970) *Journal of Catalysis* **18**, p.46-51
[34] Levy & Boudart (1974) *Journal of Catalysis*, **32**, p.304-314
[35] P. Chen, X. Wu, J. Lin, K. L. Tan (1999) *Science,* **285**, p.91-93
[36] R.T. Yang (2000) *Carbon,* **38**, p.623–641
[37] A.D. Lueking & R.T. Yang (2002) *Journal of Catalysis* **206**, p.165-168
[38] A.D. Lueking & R.T. Yang, (2004) *Applied Catalysis A: General,* **265**, p.259-268
[39] Y. Li & R.T. Yang, (2006) *Journal of the American Chemical Society*, **128**, p.726-727
[40] A.J. Lachawiec, G. Qi & R.T. Yang (2005) *Langmuir*, **21**, p.11418-11424,
[41] Y. Li & R.T. Yang (2006) *Journal of the American Chemical Society*, **128**, p.8136-8137
[42] Y. Li & R.T. Yang, (2007) *Langmuir*, **23***,* p.12937-12944
[43] Y. Y. Liu, J. L. Zeng, J. Zhang, F. Xu & L. X. Sun (2007) *International Journal of Hydrogen Energy*, **32**, p.4005-4010
[44] Y. Li & R.T. Yang (2007) *Journal of Physical Chemistry C*, **111***,* p.11086-11094
[45] M. Sabo, A. Henschel, H. Frode, E. Klemm & S. Kaskel (2007) *Journal of Materials Chemistry*, **17**, p.3827-3832
[46] Y. Li , R.T. Yang, C. Liu & Z. Wang (2007) *Industrial & Engineering Chemistry Research*, **46**, p.8277-8281
[47] R. Campesi, F. Cuevas, R. Gadiou, E. Leroy, M. Hirscher, C. Vix-guterl & M. Latroche (2008), *Carbon*, **46**, p.206-214
[48] A.J. Lachawiec & R.T. Yang (2008), *Langmuir*, **24**, p.6159-6165
[49] Y. Li & R.T. Yang (2008), *American Institute of Chemical Engineers Journal,* **54**, p.269-279
[50] A. Bourlinos, E. Kouvelos, M. A. Miller, C. Zlotea, A. Stubos & Th. Steriotis (2008**)** *Angew. Chemie*., (submitted)
[51] National Testing Laboratory for Solid-State Hydrogen Storage Technologies, DOE Annual Merit Review Meeting, Washington DC, June 9-13th, 2008
[52] C. Amorim & M.A. Keane (2008) *Journal of Colloid Interface Science,* **322**, p.196-208
[53] A.J. Lachawiec & R.T. Yang (2008), *Langmuir*, **24**, p.6159-6165.
[54] S. B. Ziemecki, G. A. Jones, D. G. Swartzfager & R. L. Harlow (1985) *Journal of the American Chemical Society*, **107**, p.4547-4548
[55] N.K. Nag (2001), *Journal of Physical Chemistry B,* **105**, p.5945
[56] N. Krishnankutty, J. Li & M. Albert Vannice (1998), *Applied Catalysis A: General,* **173**, p.137-144
[57] L. Wang & R.T. Yang (2008) *Energy & Environmental Science, Royal Society of Chemistry Cambridge, Invited Featured Review* 1, 268
[58] M. Zielinski, R. Wojcieszak, S. Monteverdi, M. Mercy & M. Bettahar (2005) *Catalysis Communications,* **6**, p.777-783
[59] R. Zacharia, K.Y. Kim, A.K.M. Fazle Kibria & K.S. Nahm (2005) *Chemical physics letters,* **412**, p.369-375
[60] Y. Li & R.T. Yang (2007) *Journal of Physical Chemistry C***, 111***,* p.11086-11094

[61] N.J. Creamer, I.P. Mikheenko, P. Yong, K. Deplanche, D. Sanyahumbi, J. Wood, K. Pollmann, M. Merroun, S. Selenska-Pobell & L.E. Macaskie (2007) *Catalysis Today,* **128**, p.80-87
[62] http://gow.epsrc.ac.uk/ViewGrant.aspx?GrantRef=EP/F027133/1, *accessed January 2009*
[63] I. de Vargas, L.E. Macaskie & E. Guibal (2004), *Journal of Chemical Technology and Biotechnology*, **79**, p.49-56
[64] W. de Windt, N. Boon, J. Van den Bulcke, L. Rubberecht, F. Prata, J. Mast, T. Hennebel & W. Verstraete (2006), *Antonie van Leeuwenhoek,* **90**, p.377-389
[65] http://pubs.usgs.gov/of/2001/of01-041/htmldocs/images/xrdschem.jpg, *accessed August 2008*
[66]http://www.globalspec.com/FeaturedProducts/Detail/Micromeritics/AccuPyc_II_1340_Series_Gas_Pycnometers/42148/0?deframe=1, *accessed August 2008*
[67] G.E. Gdowski, T.E. Felter & R.H. Stulen (1987) *Surface Science,* **181**, p.147-155
[68] A.G. Wong-Foy, A.J. Matzger & O.M. Yaghi, (2006) *Journal of the American Chemical Society*, **128**, p. 3494.
[69] L. Schlapbach & A. Zuttel (2001), *Nature*, **414**, p. 353-358
[70] M.A. Miller, C. Wang & G.N. Merrill (2009) *Journal of Physical Chemistry C*, **113***,* p.3222–3231
[71] H.W. Langmi, D. Book, A. Walton, S.R. Johnson, M.M. Al-Mamouri, J.D. Speight, P.P. Edwards, I.R. Harris, P.A. Anderson (2005) *Journal of Alloys and Compounds* 404–406 p. 637–642
[72] N.J. Creamer, I.P. Mikheenko, P. Yong, K. Deplanche, D. Sanyahumbi, J. Wood, K. Pollmann, M. Merroun, S. Selenska-Pobell & L.E. Macaskie (2007) *Catalysis Today,* **128**, p.80-87